

**SIGNAL ACQUISITION AND TRACKING FOR A SOFTWARE GPS RECEIVER**

Sophia Y. Zheng

A THESIS SUBMITTED TO THE FACULTY OF THE VIRGINIA POLYTECHNIC  
INSTITUTE AND STATE UNIVERSITY IN PARTIAL FULFILLMENT OF THE  
REQUIREMENTS FOR THE DEGREE OF

MASTER OF SCIENCE

IN

ELECTRICAL ENGINEERING

WAYNE A. SCALES, CHAIRMAN  
IRA JACOBS  
TIM PRATT

FEBURARY, 2005  
BLACKSBURG, VIRGINIA

KEYWORDS: GPS, GPS SOFTWARE RECEIVER, GPS SIMULATOR GSS 6560  
ACQUISITION, TRACKING, BASS METHOD

# SIGNAL ACQUISITION AND TRACKING FOR A SOFTWARE GPS RECEIVER

Sophia Y. Zheng

## (ABSTRACT)

Global Positioning System (GPS) is a satellite-based navigation system that has been used widely both in civilian and military for positioning, navigation, timing and other position related applications. The hardware-based GPS receivers provide the least user flexibility. Thus, it is necessary to have Software-based GPS receivers for easy and quick implementation, simulation and analysis of algorithms. Software-based GPS receiver processes the GPS signal at the radio frequency or intermediate frequency depending on the hardware configuration of the receiver. In this development of the acquisition and tracking processes of the software receiver, the front-end device that converts the radio frequency signal from the antenna to an intermediate frequency is the Mitel 2021 GPS receiver board. An analog-to-digital (A/D) converter then digitizes the output signal from the RF front-end. The data is then processed using MATLAB programs to achieve acquisition and tracking of the GPS signals. The software GPS receiver can perform acquisition and tracking using different parameters and threshold values. This flexibility of operation allows weaker signals to be tracked and processed.

In this software receiver design, the focus is on the acquisition and tracking of L1 band C/A code GPS signals used by most civilian applications. The purpose of this thesis is to develop the acquisition and tracking algorithms to extract the navigation data bits from the raw GPS signals. The navigation data bits provide all the necessary information to compute the pseudorange between the receiver and the visible satellites and determine the receiver location. Both MATLAB simulated GPS data and realistic GPS signals from a GSS 6560 simulator are used to verify the performance of the acquisition and tracking programs. The acquisition program is capable of locating the beginning of the C/A code and the carrier frequency to within the desired accuracy. From the output of the acquisition program, the tracking program can decode the navigation data bits. The tracking algorithm implemented is based on the block adjustment of synchronizing signal (BASS) method.

## ACKNOWLEDGEMENTS

I would like to begin by thanking my advisor and committee chair, Dr. Wayne Scales, for giving me the opportunity to research this thesis topic and for all the advice and guidance that he has given me over the course of my research. Without him, the completion of my thesis would have been impossible. Also, I would like to thank Dr. Ira Jacobs and Dr. Tim Pratt for serving on my committee. I would also like to thank Tsung-Cheng Wu and Chen Chen for their help in the GPS Laboratory and contributing to my research. Finally, I would like to thank all my friends who have given me assistance and support during my studies.

# TABLE OF CONTENTS

ABSTRACT .....	II
ACKNOWLEDGEMENTS .....	III
TABLE OF CONTENTS .....	IV
LIST OF FIGURES .....	V
LIST OF TABLES .....	VII
CHAPTER 1 INTRODUCTION .....	1
1.1 HISTORY OF GPS .....	1
1.2 STRUCTURE OF GPS.....	2
1.2.1 <i>The Control Segment</i> .....	2
1.2.2 <i>The Space Segment</i> .....	3
1.2.3 <i>The User Segment</i> .....	4
1.3 USER POSITION SOLUTION .....	4
1.3.1 <i>Solution of User Position From Pseudorange Measurements</i> .....	4
1.3.2 <i>User Position Accuracy Measure</i> .....	5
CHAPTER 2 GPS SIGNAL STRUCTURE.....	5
2.1 GPS SIGNAL STRUCTURE.....	6
2.2 THE P CODE.....	7
2.3 THE C/A CODE.....	7
2.4 GENERATION OF C/A CODE .....	9
2.5 CORRELATION PROPERTIES OF C/A CODE.....	11
2.6 NAVIGATION DATA MESSAGE .....	14
2.7 DOPPLER SHIFT.....	15
CHAPTER 3 SOFTWARE GPS RECEIVER.....	18
3.1 ADVANTAGES OF A SOFTWARE GPS RECEIVER.....	18
3.2 SOFTWARE RECEIVER ARCHITECTURE.....	19
3.3 SOFTWARE RECEIVER INPUT SIGNALS .....	20
3.3.1 <i>Simulated Ideal GPS Signal in MATLAB</i> .....	20
3.3.2 <i>RF Signal from GSS 6560 Signal Simulator</i> .....	24
CHAPTER 4 GPS C/A CODE SIGNAL ACQUISITION.....	26
4.1 FACTORS AFFECTING THE ACQUISITION PERFORMANCE.....	27
4.1.1 <i>Data Length for Acquisition</i> .....	27
4.1.2 <i>Doppler Frequency Search Step</i> .....	28
4.2 ACQUISITION METHODS.....	28
4.2.1 <i>Serial Search in the Time Domain</i> .....	29
4.2.2 <i>Parallel Search in the Frequency Domain using FFT</i> .....	30
4.2.3 <i>Fine Carrier Frequency Resolution</i> .....	33
4.3 PERFORMANCE OF THE ACQUISITION PROGRAM .....	35
CHAPTER 5 TRACKING OF GPS C/A CODE SIGNAL.....	39
5.1 CODE TRACKING.....	40
5.1.1 <i>The Early, Prompt and Late Codes</i> .....	40
5.1.2 <i>The Delay-Locked Loop (DLL)</i> .....	41
5.2 CARRIER TRACKING .....	42
5.2.1 <i>The Phase-Locked Loop (PLL)</i> .....	42
5.3 GPS SIGNAL TRACKING USING THE BASS METHOD .....	44
CHAPTER 6 FUTURE WORK.....	52
LIST OF REFERENCES.....	53

## LIST OF FIGURES

<a href="#"><u>FIGURE 1.1 THE THREE SEGMENTS OF GPS</u></a> .....	2
<a href="#"><u>FIGURE 1.2 GPS SATELLITE CONSTELLATION</u></a> .....	4
<a href="#"><u>FIGURE 2.1 BIPHASE MODULATION OF GPS SIGNAL</u></a> .....	5
<a href="#"><u>FIGURE 2.2 GENERATION OF GPS L1 FREQUENCY SIGNAL</u></a> .....	7
<a href="#"><u>FIGURE 2.3 POWER SPECTRUM OF SIMULATED C/A CODED GPS L1 FREQUENCY SIGNAL</u></a> ....	8
<a href="#"><u>FIGURE 2.4 POWER SPECTRUM OF C/A CODE OF SATELLITE 31 SAMPLED AT 5 MHZ</u></a> .....	8
<a href="#"><u>FIGURE 2.5 GPS C/A CODE GENERATOR</u></a> .....	9
<a href="#"><u>FIGURE 2.6 A THE AUTOCORRELATION OF SATELLITE 15</u></a> .....	12
<a href="#"><u>FIGURE 2.6 B THE AUTOCORRELATION OF SATELLITE 15 (CLOSE-UP)</u></a> .....	12
<a href="#"><u>FIGURE 2.7 THE CROSS-CORRELATION OF SATELLITE 15 AND SATELLITE 31</u></a> .....	13
<a href="#"><u>FIGURE 2.7 DOPPLER VELOCITY VS. ELEVATION ANGLE</u></a> .....	16
<a href="#"><u>FIGURE 3.1 SOFTWARE RECEIVER ARCHITECTURE</u></a> .....	19
<a href="#"><u>FIGURE 3.2 SOFTWARE RECEIVER RF FRONT-END SETUP</u></a> .....	19
<a href="#"><u>FIGURE 3.3 SIMULATED GPS NAVIGATION DATA BITS</u></a> .....	20
<a href="#"><u>FIGURE 3.4 SAMPLED GPS C/A CODE FOR SATELLITE 11</u></a> .....	21
<a href="#"><u>FIGURE 3.5 POWER SPECTRUM OF GPS C/A CODE FOR SATELLITE 11</u></a> .....	21
<a href="#"><u>FIGURE 3.6 SIMULATED BASEBAND GPS C/A CODED DATA FOR SATELLITE 11</u></a> .....	22
<a href="#"><u>FIGURE 3.7 POWER SPECTRUM OF SIMULATED IF SIGNAL</u></a> .....	22
<a href="#"><u>FIGURE 3.8 SPECTRUM OF SIMULATED GPS C/A CODED DATA FOR SATELLITE 11 AT IF</u></a> ....	23
<a href="#"><u>FIGURE 3.9 A SIMULATED BASEBAND GPS C/A CODED DATA FOR SATELLITE 11 AT IF</u></a> .....	23
<a href="#"><u>FIGURE 3.9 B SIMULATED BASEBAND GPS C/A CODED DATA FOR SATELLITE 11 AT IF (CLOSE-UP)</u></a> .....	24
<a href="#"><u>FIGURE 3.10 GPS SIMULATORS HARDWARE SETUP</u></a> .....	25
<a href="#"><u>FIGURE 3.11 SCREEN SHOT OF SIMGEN SCENARIO</u></a> .....	26
<a href="#"><u>FIGURE 4.1 ALGORITHM FOR SERIAL SEARCH ACQUISITION</u></a> .....	29
<a href="#"><u>FIGURE 4.2 LINEAR SEARCH ALGORITHM</u></a> .....	30
<a href="#"><u>FIGURE 4.3 ALGORITHM FOR PARALLEL SEARCH FFT-BASED METHOD ACQUISITION</u></a> .....	32
<a href="#"><u>FIGURE 4.4 ACQUISITION OF SATELLITE 11 AT IF 4.3097 MHZ</u></a> .....	35
<a href="#"><u>FIGURE 4.5 THE CORRELATION OUTPUT OF INPUT SIGNAL AND THE C/A CODE OF SATELLITE 15</u></a> .....	36
<a href="#"><u>FIGURE 4.6 FREQUENCY COMPONENT OF THE DESPREAD SIGNAL OF SATELLITE 15</u></a> .....	36
<a href="#"><u>FIGURE 4.7 A RAW GPS INPUT SIGNAL FROM SATELLITE 15 AT IF</u></a> .....	37
<a href="#"><u>FIGURE 4.7 B RAW GPS INPUT SIGNAL FROM SATELLITE 15 AT IF (CLOSE-UP)</u></a> .....	37
<a href="#"><u>FIGURE 4.8 ACQUISITION OF SATELLITE 15 AT IF 4.31 MHZ</u></a> .....	38
<a href="#"><u>FIGURE 4.9 THE CORRELATION OUTPUT OF INPUT SIGNAL AND THE C/A CODE OF SATELLITE 15</u></a> .....	38
<a href="#"><u>FIGURE 4.10 FREQUENCY COMPONENT OF THE DESPREAD SIGNAL OF SATELLITE 15</u></a> .....	39
<a href="#"><u>FIGURE 5.1 IDEAL CORRELATION OF C/A CODE AND INPUT SIGNAL</u></a> .....	40

<a href="#"><u>FIGURE 5.2 CORRELATION OF C/A CODE AND AN INPUT SIGNAL WITH PHASE SHIFT TO THE LEFT</u></a> .....	40
<a href="#"><u>FIGURE 5.3 CORRELATION OF C/A CODE AND AN INPUT SIGNAL WITH PHASE SHIFT TO THE RIGHT</u></a> .....	40
<a href="#"><u>FIGURE 5.4 CORRELATION PLOT OF THE PROMPT, EARLY, AND LATE CODES</u></a> .....	41
<a href="#"><u>FIGURE 5.5 BLOCK DIAGRAM OF CODE TRACKING LOOP</u></a> .....	42
<a href="#"><u>FIGURE 5.6 BLOCK DIAGRAM OF CARRIER TRACKING LOOP</u></a> .....	44
<a href="#"><u>FIGURE 5.7 BLOCK DIAGRAM OF CODE AND CARRIER TRACKING LOOPS</u></a> .....	45
<a href="#"><u>FIGURE 5.8 SPECTRUM OF RECEIVED GPS C/A CODED DATA FOR SATELLITE 11 AT IF</u></a> .....	46
<a href="#"><u>FIGURE 5.9 SPECTRUM OF RECEIVED GPS SIGNAL FOR SATELLITE 11 WITH C/A CODE REMOVED</u></a> .....	47
<a href="#"><u>FIGURE 5.10 SPECTRUM OF RECEIVED GPS SIGNAL FOR SATELLITE 11 WITH C/A CODE AT BASEBAND</u></a> .....	47
<a href="#"><u>FIGURE 5.11 SPECTRUM OF RECEIVED GPS SIGNAL FOR SATELLITE 11 AT BASEBAND</u></a> .....	48
<a href="#"><u>FIGURE 5.12 RECOVERED GPS NAVIGATION DATA BITS FOR SATELLITE 11</u></a> .....	48
<a href="#"><u>FIGURE 5.13 SPECTRUM OF RECEIVED GPS C/A CODED DATA FOR SATELLITE 15 AT IF</u></a> .....	49
<a href="#"><u>FIGURE 5.14 SPECTRUM OF RECEIVED GPS SIGNAL FOR SATELLITE 15 WITH C/A CODE REMOVED</u></a> .....	49
<a href="#"><u>FIGURE 5.15 SPECTRUM OF RECEIVED GPS SIGNAL FOR SATELLITE 15 WITH C/A CODE AT BASEBAND</u></a> .....	50
<a href="#"><u>FIGURE 5.16 SPECTRUM OF RECEIVED GPS SIGNAL FOR SATELLITE 15 AT BASEBAND</u></a> .....	50
<a href="#"><u>FIGURE 5.17 RECOVERED GPS NAVIGATION DATA BITS FOR SATELLITE 15</u></a> .....	51
<a href="#"><u>FIGURE 5.18 A RECOVERED GPS NAVIGATION DATA BITS FOR SATELLITE 15 FOR 400 MS</u></a>	51
<a href="#"><u>FIGURE 5.18 B RECOVERED GPS NAVIGATION DATA BITS FOR SATELLITE 15 FOR 400 MS</u></a>	52

## LIST OF TABLES

<u>TABLE 1.1 CHARACTERISTICS OF GPS SATELLITES</u> .....	3
<u>TABLE 2.1 GPS C/A CODE PHASE ASSIGNMENT</u> .....	10
<u>TABLE 2.2 OCCURRENCE OF CROSS-CORRELATION OF C/A CODE</u> .....	13
<u>TABLE 2.3 GPS NAVIGATION MESSAGE IN EACH SUBFRAME</u> .....	14
<u>TABLE 3.1 VALUE OF SIMULATED GPS NAVIGATION DATA BITS</u> .....	20

## CHAPTER 1 INTRODUCTION

For a long time in history, people have been searching for a reliable way to determine their location and destinations. The Global Positioning System (GPS) is the newest achievement in this search for precise positioning. Though originally intended for military use, GPS has been found useful in many civilian applications including surveying and navigation exceeding its original purpose.

### 1.1 History of GPS

The launch of Sputnik in 1957 also marked the beginning of the era of satellite navigation. Initially, the U.S. Navy developed a satellite navigation system called Transit. In 1964 Transit became functional for U.S submarines and went commercial in 1967. However, the system could only be used to calculate the position of low velocity, surface vehicles. To accommodate the need for high dynamic, high velocity vehicles such as aircrafts, GPS was eventually developed based on the concepts for the Transit system.

Since the introduction of GPS, the system has integrated into people's lives. For civilian users, GPS is generally used as a navigation tool. Whereas for military users, GPS plays a vital part in military operations that require precise and definite location readings. Therefore, GPS usage is very wide and depends on the individual user's application. Civil receivers through out the world are capable of using Standard Positioning Service (SPS) signal, while only authorized users can have Precise Positioning Service (PPS). GPS is the only system today that provides precise position information at any time, any where, and in any weather. Public transport nowadays uses GPS for navigation and receiving message from their control center.

The first GPS satellite was launched in 1978. The first ten satellites launched were developmental satellites, called Block I. From 1989 to 1997, 28 production satellites, called Block II, were launched. The last 19 satellites of this series of satellites were called Block IIA, which were the updated versions. The initial operational capability of GPS was established in December 1993. The primary system was completed with the launch of the 24th GPS satellite in 1994. In February 1994, the Federal Aviation Agency (FAA) declared GPS ready for aviation use [1]. The third-generation satellite, Block IIR, was first launched in 1997. These satellites are being used to replace the aging satellites currently in the GPS constellation. Figure 1.1 shows a picture of the IIR satellite in space. The next generation of satellites, Block IIF, is scheduled for its first launch in late 2005.

A GPS satellite provides a platform for radio transmitter, atomic clocks, computers, and various equipment used for positioning and other military projects. Each satellite broadcasts messages that allow the user to recognize the satellite and determine its position in space. The GPS system is capable of providing real-time navigation data to all users including high-dynamics users such as spacecrafts. Since the system is aimed at providing global coverage including the polar regions, the satellites must be orbiting instead of stationary. Since originally designed for military applications, the system also has some built-in tolerance for jamming signals.



## 1.2 Structure of GPS

The entire GPS system consists of three segments: the control segment, the space segment and the user segment. The control segment consists of five GPS earth stations. The master control station is located at Falcon Air Force Base in Colorado Springs, CO. The main function of the earth stations is to monitor the performance of the GPS satellites. Each monitor station has two cesium clocks as reference for the GPS system time. Each of the five earth stations makes continuous pseudorange and delta range measurements to all satellites in view every 1.5 seconds. These measurements are used to update the satellites' navigation messages. The data collected from the satellites by the earth stations is transmitted to the master control station for processing. The master control station is responsible for monitoring GPS performance, generating and uploading the navigation data to the satellites to sustain performance standards, as well as promptly detecting and responding to satellite failure to minimize the impact. Figure 1.2 is a graphical illustration of the three segments of the GPS system.

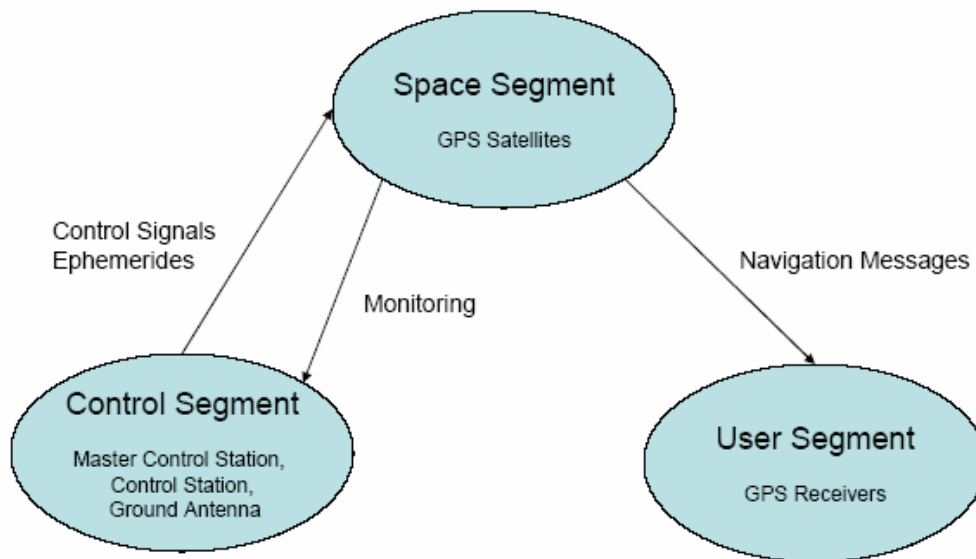


Figure 1.2 The Three Segments of GPS

### 1.2.1 The Control Segment

The locations of the GPS monitor stations are known with a high degree of accuracy and each station is equipped with a cesium atomic clock. The control segment uses the information collected by the monitor stations to predict the behavior of individual satellite's orbiting and clocking status, making sure that they remain in acceptable limits. The prediction data is up linked to the satellites for transmission back to the users. A station can perform a track up of up to 11 satellites at a time [2].

The five unmanned monitor stations are located around the world at Falcon Air Force Base in Colorado, Hawaii, Ascension Island in the Atlantic Ocean, Diego Garcia Atoll in the Indian Ocean, and Kwajalein Island in the South Pacific Ocean. The monitor stations check the exact altitude, position, speed, and the overall health of the orbiting satellites. Ground

antennas are used to monitor and track the satellites. They also transmit corrective information back to the individual satellites [2]. The signals from each satellite are read by four of the five stations excluding the station in Hawaii which does not have a ground antenna. Since the precise positions of the stations and time coordinates are known, the pseudorange measurements made by each station for a particular satellite can be used to calculate an inverted navigation solution to correct any error in the location and time of that satellite.

The measurements from the monitor stations are then sent to the master control station in Colorado. The Master Control Station is called the Consolidated Space Operations Center (CSOC), which is located at Falcon Air Force Base in Colorado Springs, Colorado. It controls the overall management of the remote monitoring and transmission sites. As the main center for support operations, the Master Control Station calculates any position or clock errors for each individual satellite according on the information received from the monitor stations. If an error is found, it passes the instructions to the monitor station with the appropriate ground antenna to relay the necessary corrective information back to that particular satellite [2]. The ephemeris of each satellite and the timing errors are uploaded to the satellites once per day via the ground antennas even without any error occurring.

### 1.2.2 The Space Segment

The space segment consists of the satellites and the Delta rockets that launch the satellites from Cape Canaveral, in Florida. Each orbit has an inclination angle (the angle between the earth's equator and the actual orbit) of  $55^\circ$  to ensure the coverage of the polar regions. The radius of the satellite orbit is 26,560 km and each satellite orbits the earth twice in one sidereal day, which is the time for the earth to complete one  $360^\circ$  rotation. The mean sidereal day is 23 hours, 56 minutes, and 4.09 seconds, which is slightly shorter than the solar day of 24 hours. Powered by solar cells, the satellites can orientate themselves to face toward the sun for power and their antennas toward the earth for transmission. Table 1.1 lists some of the characteristics of the GPS satellites.

**Table 1.1 Characteristics of GPS Satellites**

Number of Satellites	24
Number of Orbital Planes	6
Number of Satellites per Orbit	4
Orbital Inclination	$55^\circ$
Orbital Radius	26560 km
Orbital Period	11 hrs 58 min 2.05 sec
Ground Track Repeat	Sidereal Day

However, the satellites in each orbit are not evenly spaced. Two satellites are separated by  $30.0^\circ$ - $32.1^\circ$ , and the other two are  $92.38^\circ$ - $130.98^\circ$  from the first two satellites and between themselves. The spacing of the satellites minimizes the effects of a single satellite failure on system degradation [1]. The spacing of the satellites in orbit also ensures that a minimum of five satellites are in view to users worldwide with a Position Dilution of Precision (PDOP) of six or less. At any time, a receiver on Earth is capable of picking up signals from a maximum of 12 GPS satellites. A typical receiver can track between 4 to 11 satellites at a time. Most GPS receivers have a  $5^\circ$  elevation mask, which means it can only track satellites with an elevation angle greater than  $5^\circ$ . Each satellite is also equipped with an atomic clock accurate

to within three nanoseconds to let it broadcast signals that are synchronized with those from other satellites. Figure 1.4 shows a graphical representation of the GPS satellite constellation.

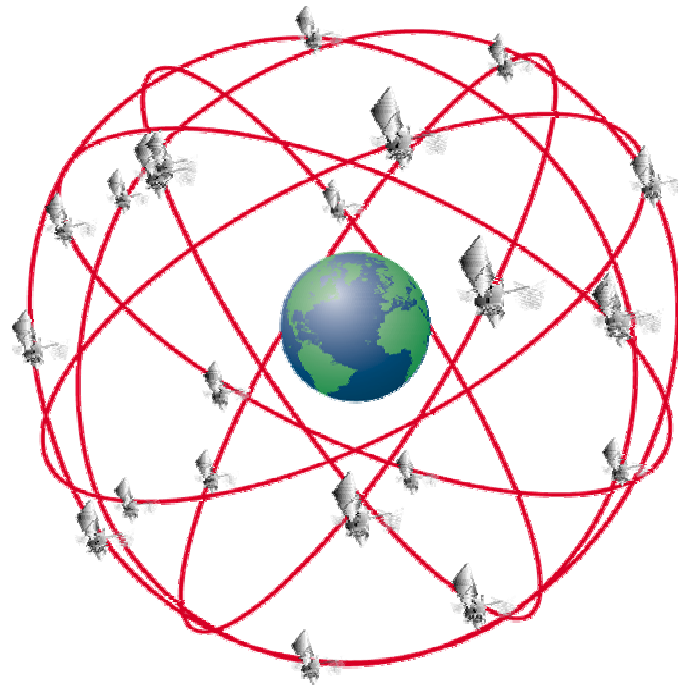


**Figure 1.4 GPS Satellite Constellation**

### **1.2.3 The User Segment**

The user segment consists of the passive GPS receivers. The receivers utilize the signals transmitted from the satellites, together with precise measurement of the signal transmission delays to determine the user position and velocity, as well as synchronize to the GPS time. The users can be classified into two groups, military and civilian users. The military uses the GPS in a wide range of scope, from navigation tools to target designation, air support to the integration of smart weapons [4]. For the civilian users, GPS is used in many applications such as point-to-point navigation as well as surveying.

## **1.3 User Position Solution**

Though the GPS signal travels to the ground at the speed of light, it still takes a measurable amount of time to reach the receiver. The receiver then calculates the distance to the satellite by measuring the difference between the time when the signal is received and the time when it was sent, and multiply by the speed of light. To calculate its precise latitude, longitude, and altitude, the receiver measures the distance to four separate GPS satellites.

### **1.3.1 Solution of User Position From Pseudorange Measurements**

To determine the user position in three-dimensional space, three satellites and three ranges from different satellites to the receiver are required. The intersection of the three distances should indicate the user's position. However, a fourth satellite is necessary to calculate the unknown bias between the satellite clock and the receiver clock. The need for

the fourth satellite is due to difference in the precise atomic clock that is used in the satellite and the normal clock used in the receiver. The atomic clock is much more accurate than the clock used in the GPS receiver. Any slight error in the user clock can result in a significant offset in the exact user location. However, the atomic clocks are much more expensive than a regular clock and it is uneconomical for every GPS receiver to contain an atomic clock. Therefore, the fourth satellite becomes necessary which allows a receiver to solve for the timing offset and eliminate it in calculating the navigation solution.

### 1.3.2 User Position Accuracy Measure

Two factors affect a user's overall position accuracy: the errors inherent in the GPS signals and the geometry of the four GPS satellites whose signals are used to calculate the navigation solution. The inherent error in the GPS signal is known as the user equivalent range error (UERE), which is primarily contributed by the clock and ephemeris errors from the satellites, atmospheric delays, multipath, and receiver noise. The other source of error depends on the GPS satellite geometry. Since the receiver determines its position using trilateration, the further apart the four satellites are, the better the receiver position accuracy is. The effect of satellite geometry on the accuracy of a navigation solution is measured by the dilution of precision (DOP).

## CHAPTER 2 GPS SIGNAL STRUCTURE

The GPS signal is a phase-modulated signal using bi-phase shift keying (BPSK). The phase change rate is often referred as the chip rate. The spectrum of the signal can be described by a sinc function with spectrum width proportional to the chip rate. If the chip rate is 1 MHz, the main lobe of the spectrum has a null-to-null width of 2 MHz. Therefore, this type of signal is referred to as a spread-spectrum signal [1]. A code division multiple access (CDMA) signal in general is a spread-spectrum system. All the signals in the system have the same carrier frequency. The signals are modulated by a set of orthogonal (or near-orthogonal) codes. In order to acquire an individual signal, the code of that signal must be used to correlate with the received signal. A system is referred as a direct-sequence modulated system when the modulation code is a digital sequence with a frequency higher than the data rate. The GPS signal is CDMA using direct sequence to bi-phase modulate the carrier frequency [1].

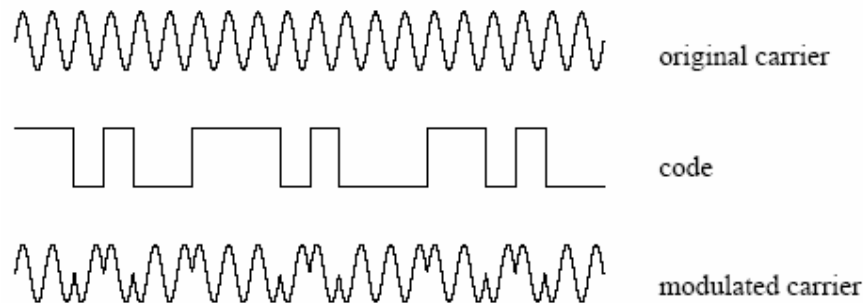


Figure 2.1 Biphase Modulation of GPS signal

Since the CDMA signals of a system use the same carrier frequency, there is a greater probability of interference among the signals. This effect is especially significant when strong and weak signals are mixed together. Sometimes during the acquisition process, a

cross-correlation peak of a strong signal may be stronger than the desired peak of a weak signal. In this case, the receiver may then obtain the wrong information. In order to avoid the interference, all the signals should have approximately the same power levels at the receiver.

## 2.1 GPS Signal Structure

There are two types of GPS signals: the coarse/acquisition (C/A) code and precision (P) code. The actual P code is encrypted by a Y code, so it is often referred as the P(Y) code. Currently, the C/A code is used for civilian applications while the P(Y) code is reserved for military use. The focus of this software GPS receiver is to acquire and track the C/A code.

The GPS signals are transmitted on two different frequencies: L1 (1575.42 MHz) and L2 (1227.6 MHz). These frequencies are coherent with a 10.23 MHz clock related as follows

$$L1 = 1575.42\text{MHz} = 154 \times 10.23\text{MHz}$$

$$L2 = 1227.6\text{MHz} = 120 \times 10.23\text{MHz}$$

There have been developments on the signal structure of GPS. Currently the L1 frequency carries both the C/A coded signals and the P(Y) signals. The L2 frequency contains only the P(Y) signal. The P(Y) code is only available for PPS users, while the C/A code is also available for SPS users. Since the focus of this software receiver design is on civilian applications, so only the acquisition and tracking GPS signals at L1 frequency are studied in detail. The GPS signal at L1 frequency can be expressed as

$$S_{L1} = A_p P(t)D(t)\cos(2\pi f_1 t + f) + A_c C(t)D(t)\sin(2\pi f_1 t + f)$$

where  $S_{L1}$  is the signal at L1 frequency,  $A_p$  is the amplitude of the P code,  $P(t) = \pm 1$  is the phase of the P code,  $D(t) = \pm 1$  is the data code,  $f_1$  is the L1 frequency,  $f$  is the initial phase,  $A_c$  is the amplitude of the C/A code,  $C(t) = \pm 1$  is the phase of the C/A code [1]. Figure 2.2 shows the block diagram of how the GPS L1 frequency signal is generated.

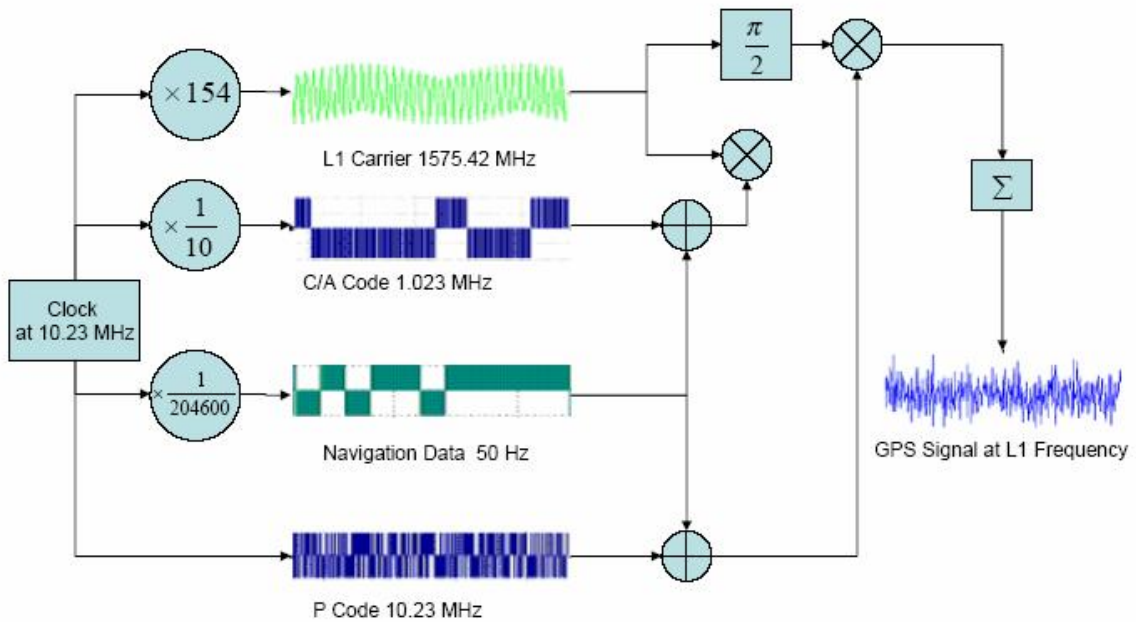


Figure 2.2 Generation of GPS L1 Frequency Signal

## 2.2 The P Code

The P code is bi-phase modulated at 10.23 MHz and the main lobe of the spectrum is 20.46 MHz wide from null-to-null. The code is generated from two pseudorandom noise (PRN) codes with the same chip rate of 10.23 MHz. One PRN sequence has 15,345,000 chips, which has a period of 1.5 seconds, the other one has 15,345,037 chips, and the difference is 37 chips. The code length generated by these two codes is 23,017,555.5 seconds, which is slightly longer than 38 weeks. However, the actual length of the P code is 1 week as the code is reset every week. This 38-week-long code can be divided into 37 different P codes and each satellite can use a different portion of the code [1]. The first 32 sets of codes are used for the satellites in orbit. Five of the P code signals (33-37) are reserved for other uses such as ground transmission. In order to perform acquisition on the signal, the time of the week information must be known very accurately which can be obtained through the C/A code.

## 2.3 The C/A Code

The C/A code is a bi-phase modulated signal with a chip rate of 1.023 MHz with a null-to-null bandwidth of the main lobe of the signal spectrum of 2.046 MHz. Each chip period is 977.5 ns (1/1.023 MHz). However, the transmission bandwidth of the GPS signal at the L1 frequency is approximately 20 MHz to accommodate the bandwidth needed for the P code signal. Therefore, in addition to the main lobe of the C/A code signal, several side lobes of the signal are also transmitted in this bandwidth. Figure 2.3 shows a screen shot of a C/A coded GPS signal on the spectrum analyzer. The L1 frequency GPS signal contains only the C/A code and is simulated by the Spirent GSS 6560 simulator. It can be observed that the null-to-null bandwidth of main lobe is approximately 2 MHz.

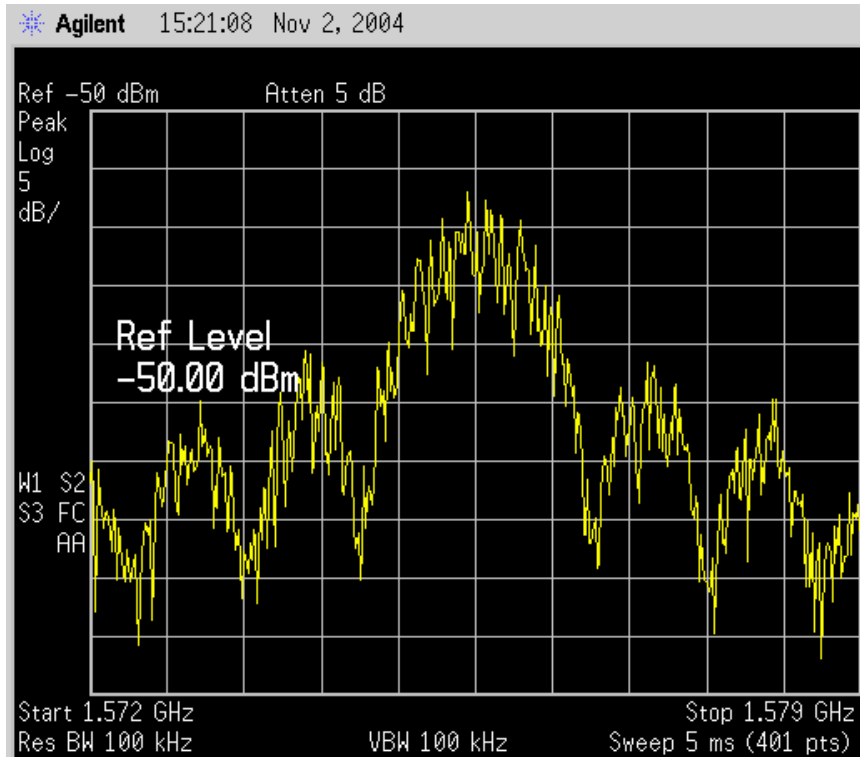


**Figure 2.3 Power Spectrum of Simulated C/A Coded GPS L1 Frequency Signal**

The spectrum of the C/A code of satellite 31 sampled at 5 MHz is shown in Figure 2.4. The C/A code period contains 1,023 chips, and with the chip rate of 1.023 MHz, the code period is 1 ms. Since the navigation data has a data rate of 50 Hz, one data bit period is 20 ms long and contains 20 complete sets of C/A codes.

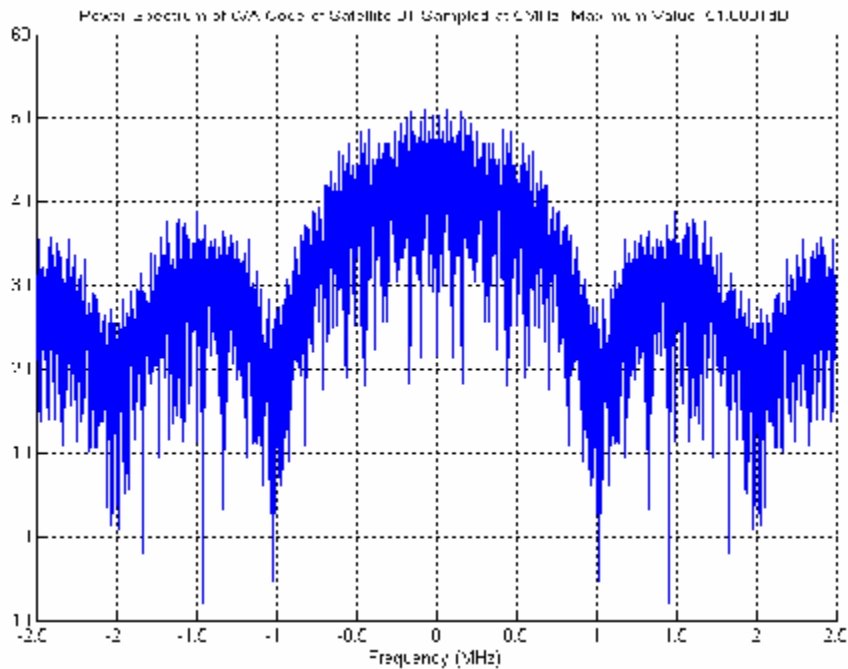


**Figure 2.4 Power Spectrum of C/A Code of Satellite 31 Sampled at 5 MHz**

## 2.4 Generation of C/A Code

To understand the acquisition and tracking of the C/A coded GPS signal, the composition of the C/A code is studied. The GPS C/A code is one kind of Pseudorandom noise (PRN) codes also known as the Gold codes. Two maximum-length linear feedback shift register (LFSR) of 10 stages, G1 and G2, driven by a 1.023 MHz clock, are used to generate a maximum length pseudo random code. If the shift register has  $n$  bits, the length of the sequence generated is  $2^n - 1$ . Since both shift registers in G1 and G2 have 10 bits, the sequence length generated is  $(2^{10} - 1) = 1023$  bits. Both G1 and G2 are initialized to be all ones, since the all-zero state is illegal. The feedback taps of the G1 and G2 LFSRs are defined by the generator polynomials

$$\begin{aligned} G1(X) &= 1 + X^3 + X^{10} \\ G2(X) &= 1 + X^2 + X^3 + X^6 + X^8 + X^9 + X^{10} \end{aligned} \quad \text{Eq. 2.1}$$

The output of the G2 LFSR for each C/A code is delayed by the modulo-2 addition of two code phase selection bits specific for each satellite. The C/A code is generated by the modulo-2 addition of the output of the G1 LFSR and the delayed output of the G2 LFSR. Figure 2.5 is a graphical presentation of how the C/A code for a particular satellite is generated. This will work since adding a phase-shifted version of a PRN sequence to itself will shift the phase of the code, while not changed the code [3]. The positions of the code selection bits determine the satellite identification. There are 32 sets of unique C/A codes for the 32 satellite numbers. Another five are reserved for various applications such as ground transmission.

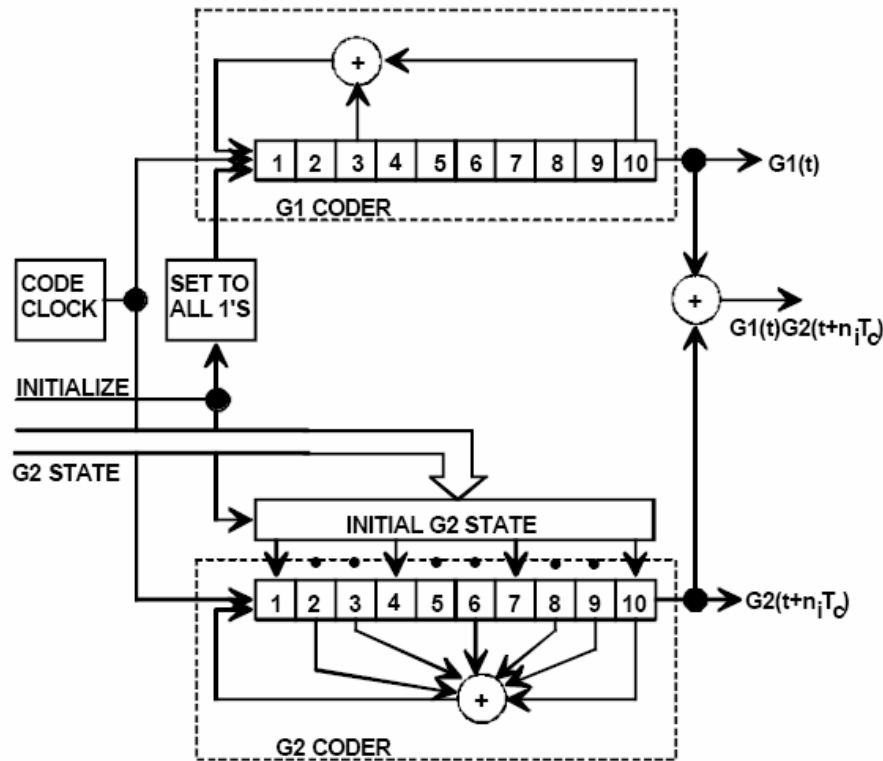


Figure 2.5 GPS C/A Code Generator



The code phase assignment of the GPS satellites are given in the Table 2.1. The satellite vehicle identification number is in column one. The second column contains the PRN number of the satellites from 1 to 37. The code phase selections of the G2 generator of the satellites are listed in column three. The code delays measured in chips are presented in column four. The last column shows the first 10 bits of the C/A code generated for each satellite in octal format.

**Table 2.1 GPS C/A Code Phase Assignment**

Satellite Vehicle ID	GPS Signal PRN	Code Phase Selection	Code Chip Delay	First 10 C/A Chips in Octal
1	1	2 ⊕ 6	5	1440
2	2	3 ⊕ 7	6	1620
3	3	4 ⊕ 8	7	1710
4	4	5 ⊕ 9	8	1744
5	5	1 ⊕ 9	17	1133
6	6	2 ⊕ 10	18	1455
7	7	1 ⊕ 8	139	1131
8	8	2 ⊕ 9	140	1454
9	9	3 ⊕ 10	141	1626
10	10	2 ⊕ 3	251	1504
11	11	3 ⊕ 4	252	1642
12	12	5 ⊕ 6	254	1750
13	13	6 ⊕ 7	255	1764
14	14	7 ⊕ 8	256	1772
15	15	8 ⊕ 9	257	1775
16	16	9 ⊕ 10	258	1776
17	17	1 ⊕ 4	469	1156
18	18	2 ⊕ 5	470	1467
19	19	3 ⊕ 6	471	1633
20	20	4 ⊕ 7	472	1715
21	21	5 ⊕ 8	473	1746
22	22	6 ⊕ 9	474	1763
23	23	1 ⊕ 3	509	1063
24	24	4 ⊕ 6	512	1706
25	25	5 ⊕ 7	513	1743
26	26	6 ⊕ 8	514	1761
27	27	7 ⊕ 9	515	1770
28	28	8 ⊕ 10	516	1774
29	29	1 ⊕ 6	859	1127
30	30	2 ⊕ 7	860	1453
31	31	3 ⊕ 8	861	1625
32	32	4 ⊕ 9	862	1712
**	33	5 ⊕ 10	863	1745
**	34	4 ⊕ 10	950	1713
**	35	1 ⊕ 7	947	1134
**	36	2 ⊕ 8	948	1456
**	37	4 ⊕ 10	950	1713

## 2.5 Correlation Properties of C/A Code

One of the most important properties of the C/A codes is their high autocorrelation peak and low cross-correlation peaks. However, in order to detect the presence of a weak signal, the peak of the autocorrelation of the weak signal must be stronger than the cross-correlation peaks of the strong signals. Theoretically if the codes are orthogonal, the cross correlation values will be zero. However, the Gold codes are only near orthogonal codes, so the cross correlation values of the C/A codes are not zero but rather small values.

The autocorrelation function of a C/A code is

$$R_{ii}(t) = \int_{-\infty}^{\infty} CA_i(t)CA_i(t+t)dt \quad \text{Eq. 2.2}$$

where  $CA_i$  is the C/A code from the  $i$ -th satellite, and  $t$  is the phase of the time shift. The correlation peak repeats every code period. The high correlation peak property of the autocorrelation function is used to synchronize the receiver locally generated code with the code of the received signal. The ideal cross-correlation of orthogonal codes are zero, but since the C/A codes are only near orthogonal, the cross-correlation values are not zero but small compared to the correlation peak value. The cross-correlation between the C/A codes of two satellites is defined as

$$R_{ij}(t) = \int_{-\infty}^{\infty} CA_i(t)CA_j(t+t)dt \quad \text{Eq. 2.3}$$

where  $CA_i$  is the C/A code for the  $i$ -th satellite and  $CA_j$  is the C/A code for the  $j$ -th satellite and  $i \neq j$ .

In Figure 2.6 a, the autocorrelation of one set of C/A code for satellite 15 is plotted. A close-up view of the autocorrelation is shown in Figure 2.6 b. The maximum autocorrelation value is 1023, which corresponds to the number of chips in one set of the C/A code. The scale of the figure is shifted to show the peak at the center. The autocorrelation reaches its maximum when  $t = 0$ .

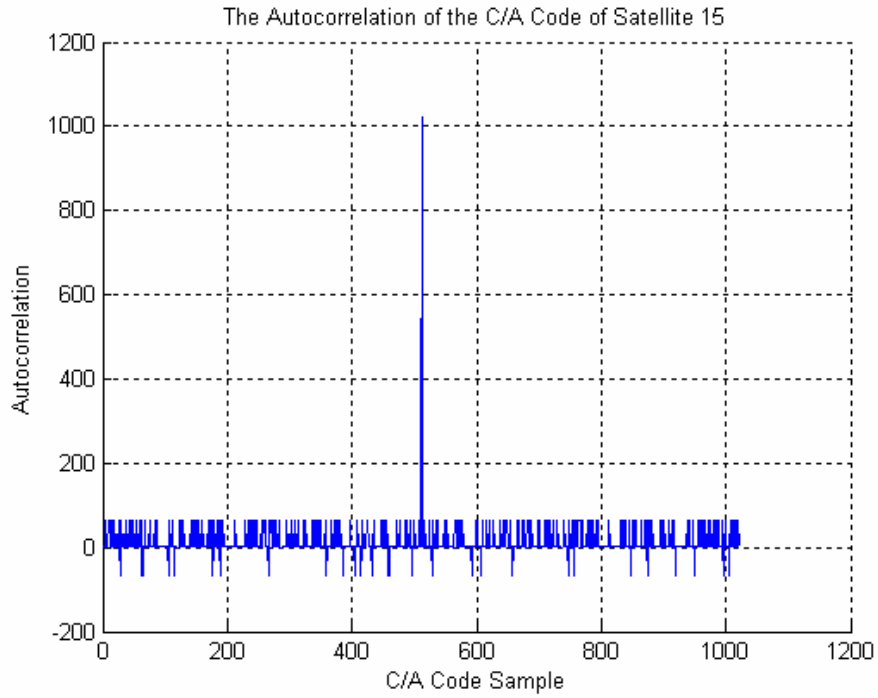


**Figure 2.6 a The Autocorrelation of Satellite 15**

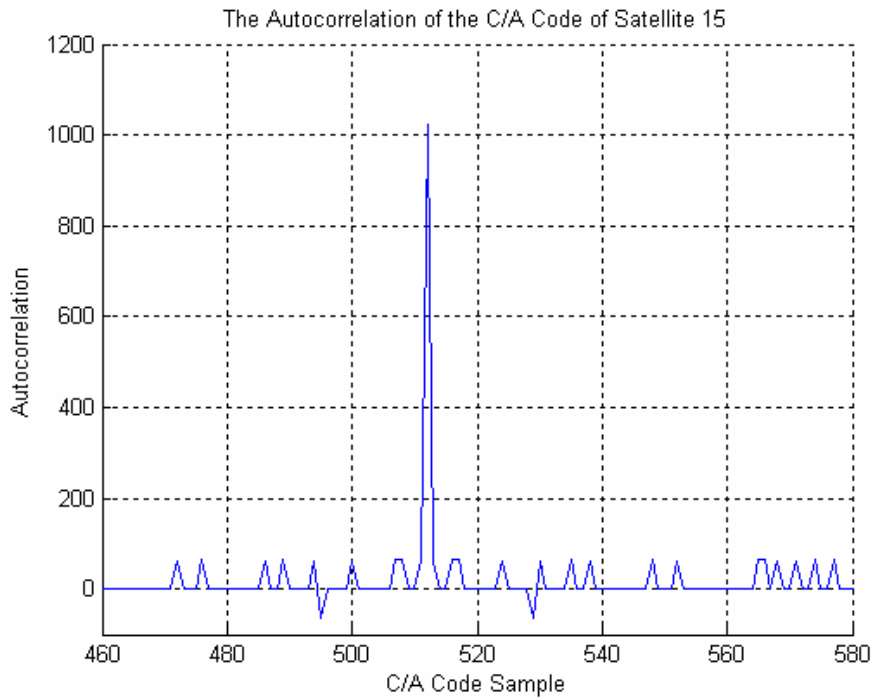


**Figure 2.6 b The Autocorrelation of Satellite 15 (Close-up)**

The cross-correlation value of two Gold Codes with even  $n$  values is one of the three values calculated using Eq. 2.4

$$Cross - correlation = \begin{cases} -\frac{2^{\binom{n+1}{2}} + 1}{P} \\ -\frac{1}{P} \\ \frac{2^{\binom{n+1}{2}} - 1}{P} \end{cases}, \quad \begin{matrix} P = 2^n - 1 \\ n = even \end{matrix} \quad \text{Eq. 2.4}$$

In the case of the C/A codes,  $n = 10$  is even, so the  $P$  value is calculated to be 1,023. The cross-correlation values are calculated using Eq. 2.4 and the results are given in Table 2.2.

**Table 2.2 Occurrence of Cross-Correlation of C/A Code**

Cross-Correlation Value	Occurrence (%)
-65/1023	12.5
-1/1023	75
63/1023	12.5

The cross-correlation values of the C/A codes of satellite 15 and 31 is presented in the Figure 2.7. Since the values are very small, the GPS satellites can simultaneously broadcast signals at the same frequency. The cross-correlation takes on one of the three values 63, -65 and -1 [1].

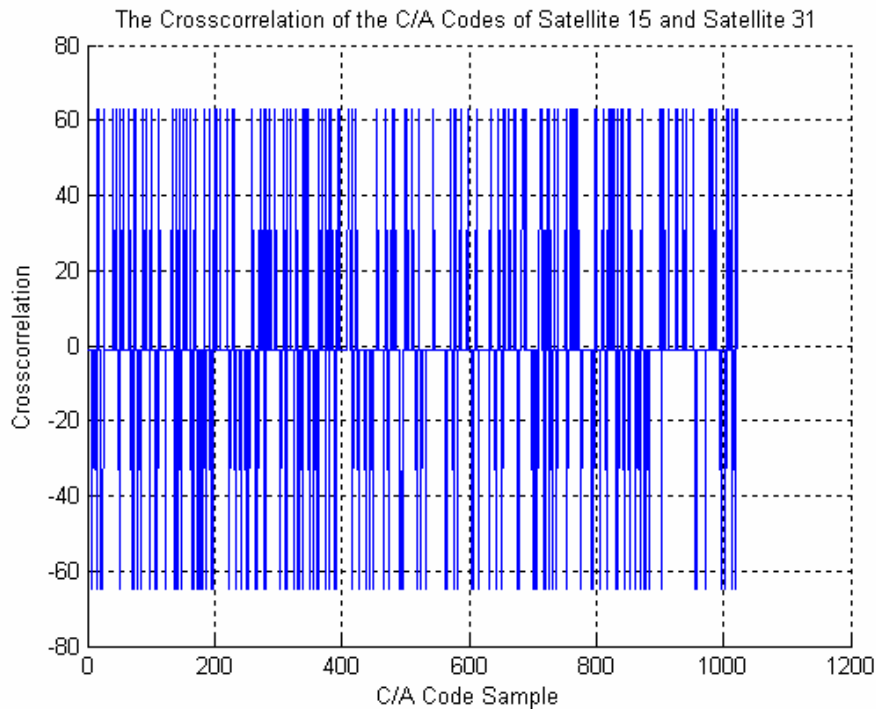


**Figure 2.7 The Cross-Correlation of Satellite 15 and Satellite 31**

From Figure 2.6 and 2.7, it can be seen that the correlation peak value is much more significant than any other correlation values. The high peak value helps the receiver to acquire the GPS signal. The secondary peaks in the autocorrelation are at least

approximately 24 dB down from the original peak. The ratios of the secondary peaks are the maximum and are calculated as follows

$$10\log\left(\left|\frac{63}{1023}\right|^2\right) = -24.2dB$$

$$10\log\left(\left|\frac{-65}{1023}\right|^2\right) = -23.9dB$$

$$10\log\left(\left|\frac{63}{1023}\right|^2\right) = -60.2dB$$

## 2.6 Navigation Data Message

GPS satellites transmit 50-bit-per-second data streams which are superimposed on the C/A- and P-codes via modulo-2 additions. Once a receiver has matched its code to the code of a satellite at the carrier frequency, it can begin to decode the navigation data message from the particular satellite. Thirty data bits make up a word which is 600 ms long. Ten words make up a subframe of 6 seconds. A page of data contains 5 subframes and is 30 seconds long. A satellite's entire data message lasts 12.5 minutes and contains 25 pages of data.

The 1500 bits navigation message contains information concerning the satellite clock, the satellite orbit, the satellite health status, and various other data. The information content of the five subframes can be summarized in Table 2.3

**Table 2.3 GPS Navigation Message in Each Subframe**

Subframe 1:	satellite clock corrections, health indicators, age of data
Subframe 2-3:	satellite ephemerides
Subframe 4:	ionosphere model parameters, UTC data, almanac and health status data for satellites numbered 25 and higher
Subframe 5:	almanac and health status data for satellites numbered 1-24

The first three subframes contain information about the ephemeris used to calculate the user position. Each subframe contains ten words. The first word is the telemetry word (TLM) containing a synchronization pattern and diagnostic messages. The second word of each subframe is the hand-over word (HOW) which contains among others the Z-count, an internally derived 1.5 s since the beginning of the current GPS week in each satellite. This number and the P-code give the reading of the satellite clock at signal transmission time. The GPS time is given in terms of the number of seconds in a week and is reset at the end/start of each week. At the end/start of the week, the cyclic paging to subframes one through five will restart with subframe one regardless of which subframe was last transmitted prior to end/start of week [1]. All upload and page cutovers will occur on frame boundaries.

Each satellite transmits its own position in three-dimensional coordinates and time. All GPS receivers are passive, so they are solely dependent on the received signals for the necessary processing. The receivers make use of one way Time of Arrival (TOA), which is the transmission time from satellites to the receivers. The navigation data provides the receiver with the location of the satellite at the time of transmit.

## 2.7 Doppler Shift

The Doppler frequency shift caused by the satellite motion affects both the carrier frequency and the C/A code. The radius of the earth is 6,378 km around the equator and 6,357 km at the poles. The mean earth radius is considered as 6,371.3 km. The angular velocity  $dq/dt$  and the speed of the satellite  $v_s$  can be calculated from the approximate radius of the satellite orbit as

$$\frac{dq}{dt} = \frac{2p}{11 \times 3600 + 58 \times 60 + 2.05} \approx 1.458 \times 10^{-4} \text{ rad/s} \quad \text{Eq. 2.5}$$

$$v_s = \frac{r_s dq}{dt} = 26560 \times 1.458 \times 10^{-4} = 3874 \text{ m/s} \quad \text{Eq. 2.6}$$

where  $r_s$  is the mean radius of the satellite orbit and  $q$  is the angle between the user and the satellite.

The Doppler frequency is caused by the satellite velocity component  $v_d$  direct toward the receiver

$$v_d = v_s \sin b = \frac{v_s r_e \cos q}{\sqrt{r_e^2 + r_s^2 - 2r_e r_s \sin q}} \quad \text{Eq. 2.7}$$

where  $r_e$  is the mean radius of the earth.

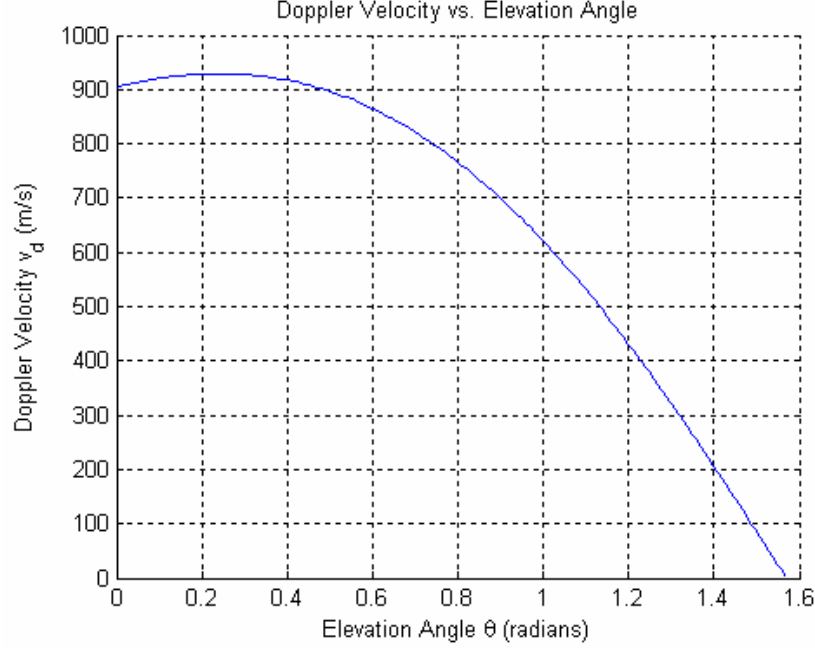


**Figure 2.7 Doppler Velocity vs. Elevation Angle**

Figure 2.7 shows the Doppler velocity is zero when the elevation angle is  $90^\circ$ . The maximum Doppler velocity is calculated by taking the derivative of the Doppler velocity and setting it equal to zero as follows [1]

$$\frac{dv_d}{dq} = \frac{v_s r_e [r_e r_s \sin^2 q - (r_e^2 + r_s^2) \sin q + r_e r_s]}{(r_e^2 + r_s^2 - 2r_e r_s \sin q)^{3/2}} = 0$$

The maximum Doppler velocity  $v_{dm}$  occurs along the horizon and is calculated using Eq. 2.8.

$$v_{dm} = \frac{v_s r_e}{r_s} = \frac{3874 \times 6371.3}{26560} = 929.3 \text{ m/s} \quad \text{Eq. 2.8}$$

The maximum Doppler frequency for the L1 frequency can therefore be calculated using Eq. 2.9

$$f_{dm} = \frac{f_r v_{dm}}{c} = \frac{1575.42 \times 10^6 \times 929.3}{2.99792458 \times 10^8} = 4.88 \text{ kHz} \quad \text{Eq. 2.9}$$

In the acquisition phase of the receiver, the search range is expanded to  $\pm 5$  kHz of the carrier frequency to accommodate Doppler Frequency shift.

The Doppler frequency also shifts the C/A code, but the effect is rather small due to the low frequency of the C/A code (1.023MHz). The Doppler frequency on the C/A code is calculated as follows

$$f_{dc} = \frac{f_c v_{dm}}{c} = \frac{1.023 \times 10^6 \times 929.3}{2.99792458 \times 10^8} = 3.17 \text{ Hz} \quad \text{Eq. 2.10}$$

The rate of change of the Doppler frequency is an important factor in determining the frequency update rate in the tracking process. One simple way to estimate the average rate of change of the Doppler frequency and another way is to calculate the maximum rate of change of the Doppler frequency [1]. The elevation angle for the maximum Doppler velocity can be solved using Eq 2.11

$$q_{\max} = \sin^{-1} \left( \frac{r_e}{r_s} \right) \approx 0.242 \text{ rad} \quad \text{Eq. 2.11}$$

Since the satellite completes one orbit in 11 hours, 58 minutes and 2.05 seconds, the satellite travels  $2p$  radians. The time it takes to change from the maximum Doppler angle to minimum Doppler angle is calculated as follows

$$t = (11 \times 3600 + 58 \times 60 + 2.05) \frac{\left( \frac{p}{2} - 0.242 \right)}{2p} = 9109.5 \text{ sec} \quad \text{Eq. 2.12}$$

During this time, the Doppler frequency changes from 4.9 kHz to 0, so the average rate of change of the Doppler frequency can be calculated as

$$df_{dr} = \frac{4.88 \times 10^3}{9109.5} = 0.536 \text{ Hz/s} \quad \text{Eq. 2.13}$$

In tracking the GPS signal in a GPS receiver, two factors are necessary to update the tracking loop: the change of the carrier frequency and the alignment of the input data signal and the locally generated C/A code. However, since the change in Doppler frequency is not constant over time, the maximum Doppler frequency change also needs to be considered. The maximum change in Doppler velocity,  $v_d$ , over time can be computed as follows [1]

$$\frac{dv_d}{dt} = \frac{dv_d}{dq} \frac{dq}{dt} = \frac{v_s r_e \left[ r_e r_s \sin^2 q - (r_e^2 + r_s^2) \sin q + r_e r_s \right] \frac{dq}{dt}}{\left( r_e^2 + r_s^2 - 2r_e r_s \sin q \right)^{3/2}} \quad \text{Eq. 2.14}$$

Since the maximum rate of change of the frequency occurs at  $q = \frac{p}{2}$ , the corresponding maximum rate of change of the speed is [1]

$$\left. \frac{dv_d}{dt} \right|_{\max} = \left. \frac{v_s r_e \frac{dq}{dt}}{\sqrt{r_e^2 + r_s^2 - 2r_e r_s \sin q}} \right|_{q=\frac{p}{2}} \approx 0.178 \text{ m/s}^2 \quad \text{Eq. 2.15}$$



The maximum rate of change of the Doppler frequency can then be calculated as

$$df_{dr}|_{\max} = \frac{dv_d}{dt} \frac{f_r}{c} = \frac{0.178 \times 1575.42 \times 10^6}{2.99792458 \times 10^8} = 0.936 \text{ Hz/s} \quad \text{Eq. 2.16}$$

This value is still relatively small which allows the tracking loop to be updated every second. From the above calculations, it can be seen that the rate of change of the Doppler frequency caused by the satellite motion is very low and the update rate of the tracking program is much more frequent for the satellite motions to have significant effects.

## CHAPTER 3 SOFTWARE GPS RECEIVER

In a conventional GPS receiver, the acquisition and tracking of the signals are all processed by the hardware. However, in a software GPS receiver, the signal is digitized using an analog-to-digital converter (ADC). The digitized input signal is then processed using the software receiver. The acquisition process searches for the presence of a signal from a particular satellite, and the tracking program finds the phase transition of the navigation data from that satellite. Ephemeris data and pseudoranges can be recovered from the navigation data bits. Finally the user position can be calculated from the ephemeris obtained.

### 3.1 Advantages of A Software GPS Receiver

A GPS software receiver has more flexibility due to its hardware independence. The receiver is mainly implemented in software except for the front-end part, which offers various advantages. First, a software receiver removes the nonlinear, temperature-dependent components of conventional hardware receivers. Second, a software receiver can provide more evaluation and testing flexibilities. Some systems may collect complex data in both the in-phase ( $I$ ) and quadrature ( $Q$ ) channels while others use real data from one channel [1]. The output data from these different platforms can be processed by the same software receiver. Both complex and real data can be generated by the software receiver with slight modifications. The software receiver can also adapt to data digitized with various sampling frequencies. The performance of different algorithms can be compared without any hardware development. Third, it provides an effective simulation environment. New algorithms can be developed for the software receiver to solve problems, such as jamming signals, without altering the hardware components. It is easy to prototype theoretical signals such as the L5 frequency signal (currently being developed by the GPS modernization program) and test the processing techniques for the new signal without any new hardware development.

The data input to the software receiver does not have to be processed in real time. Therefore the receiver does not have to be constantly tracking the signals, which is useful in cases where data cannot be collected continuously [1]. Theoretically, the minimum amount of data necessary to make the position calculations is only 18 seconds. However, with Doppler shift, the subframes from different satellites will arrive at the receiver at different times. In addition, the beginning of subframe 1 of each satellite data also needs to be obtained. In order to properly calculate the user position, at least 30 seconds of GPS data is required [1]. However, this maybe another advantage in a software receiver, where only 30 seconds of data can be used to calculate an initial user position.

### 3.2 Software Receiver Architecture

The architecture of software-based GPS receiver is as shown in Figure 3.1. It consists of an antenna and a RF front-end and an Analog-to-Digital Converter (ADC). The RF front-end device is necessary to down convert the GPS signal to an intermediate frequency (IF). The IF signal is then sampled and digitize through the ADC.

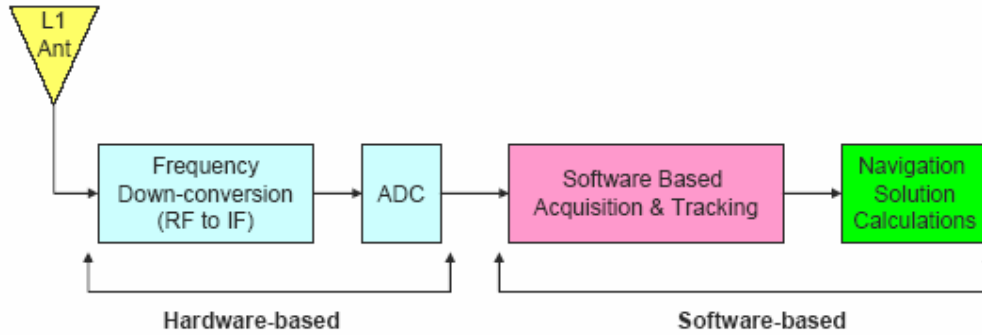


Figure 3.1 Software Receiver Architecture

The front-end of this software receiver design is through the Mitel GP2021 receiver. The GP2021 chip contains five signal down conversion stages. The first three stages are performed by mixers in the GP2010 front-end chip. The fourth down conversion is digital, occurring in the sampler which is driven by the 40/7 MHz GP2021 SAMPCLK output. The final down conversion occurs in the GP2021 correlator, where quadrature outputs of the carrier DCO are mixed with the sampled GPS IF signal to produce the in-phase and quadrature outputs I and Q at base-band. The input signal to the A/D converter is extracted from the third stage IF through an output pin. The input signal to the ADC is at an IF of approximately 4.31 MHz, and the sampling frequency is 20 MHz. The sampling frequency was chosen experimentally that has the best acquisition and tracking performance. The hardware setup used for downconverting the GPS data and the ADC are shown in Figure 3.2. The GPS signal extracted from the GP2010 output pin is shown in Figure 3.3



Figure 3.2 Software Receiver RF Front-End Setup

To recover the navigation information the digitized signal then goes through the acquisition and tracking processes implemented in software. The acquisition process searches for the presence of a signal from a particular satellite, and the tracking program finds the phase transitions of the navigation data from a particular satellite. Ephemeris data and pseudoranges can be recovered from the navigation data bits. Finally the user position can be calculated from the ephemeris obtained.

### 3.3 Software Receiver Input Signals

#### 3.3.1 Simulated Ideal GPS Signal in MATLAB

To understand the performance of the acquisition and tracking programs, 10 GPS data bits are initially simulated in MATLAB at the carrier frequency of 4.3097 MHz. Table 3.1 lists the values of each data bit and Figure 3.3 graphically illustrated the simulated navigation data.

**Table 3.1 Value of Simulated GPS Navigation Data Bits**

Bit	1	2	3	4	5	6	7	8	9	10
Value	1	-1	1	-1	1	1	-1	-1	1	-1

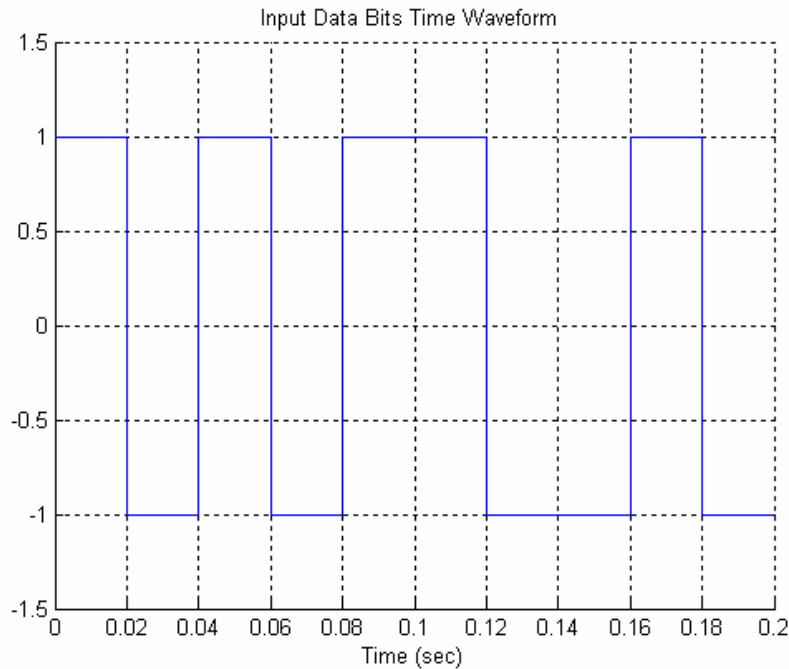


**Figure 3.3 Simulated GPS Navigation Data Bits**

As discussed previously in sections 2.3 and 2.4, the GPS navigation data is modulated with a satellite specific C/A code. The locally generated C/A code is also digitized at 20 MHz to match the sampled navigation data. Figure 3.4 illustrates the sampled C/A code for satellite 11. The power spectrum of the sampled C/A code of satellite 11 is shown in Figure 3.5. The main lobe bandwidth of the C/A code is approximately 2 MHz which corresponds to the theoretical value of 2.046 MHz. The signal is also at baseband before modulated with the carrier.

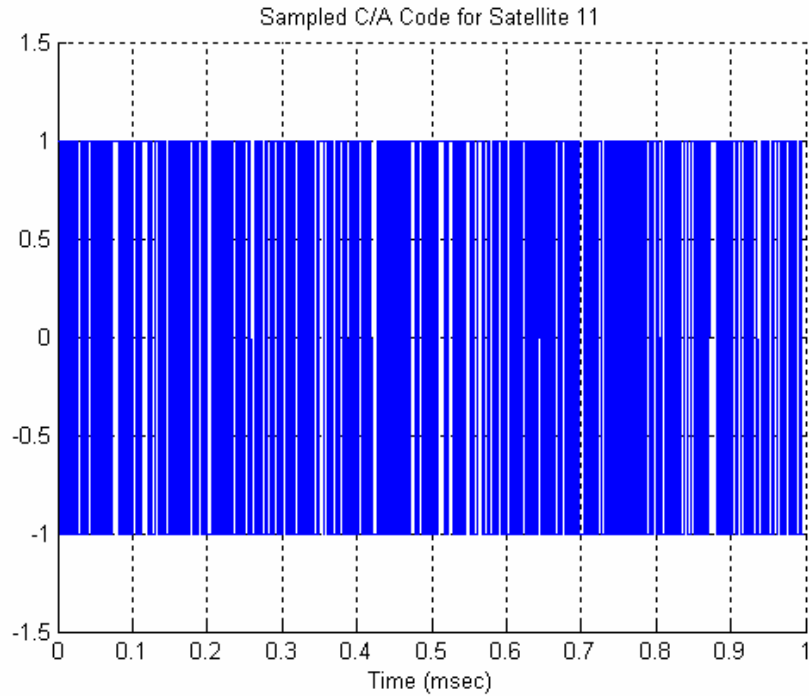


**Figure 3.4 Sampled GPS C/A Code for Satellite 11**

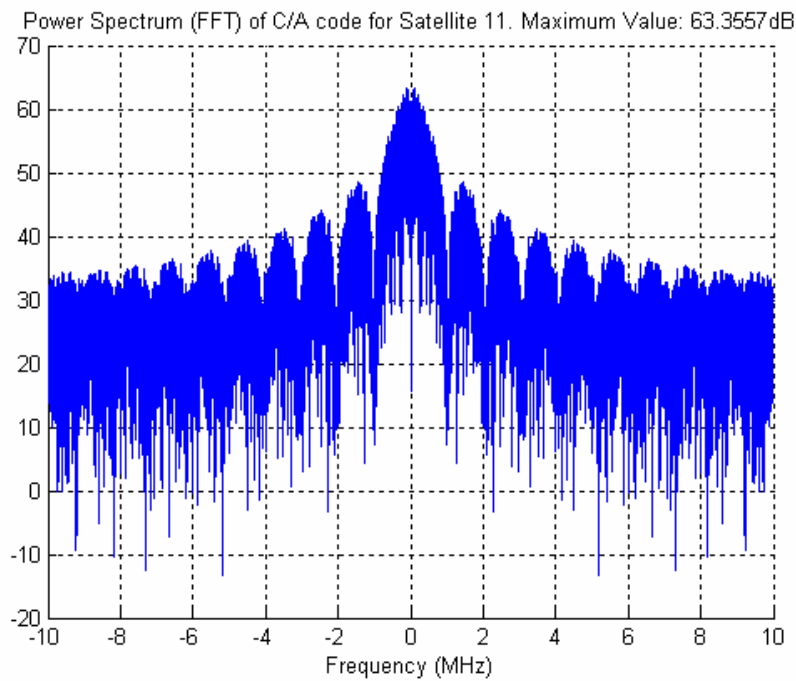


**Figure 3.5 Power Spectrum of GPS C/A Code for Satellite 11**

The input data bits are then multiplied with the digitized C/A code samples. The resulting signal is still at baseband and is shown in Figure 3.6. The figure plots the data for one millisecond which consists of one complete set of C/A codes sampled at 20 MHz.

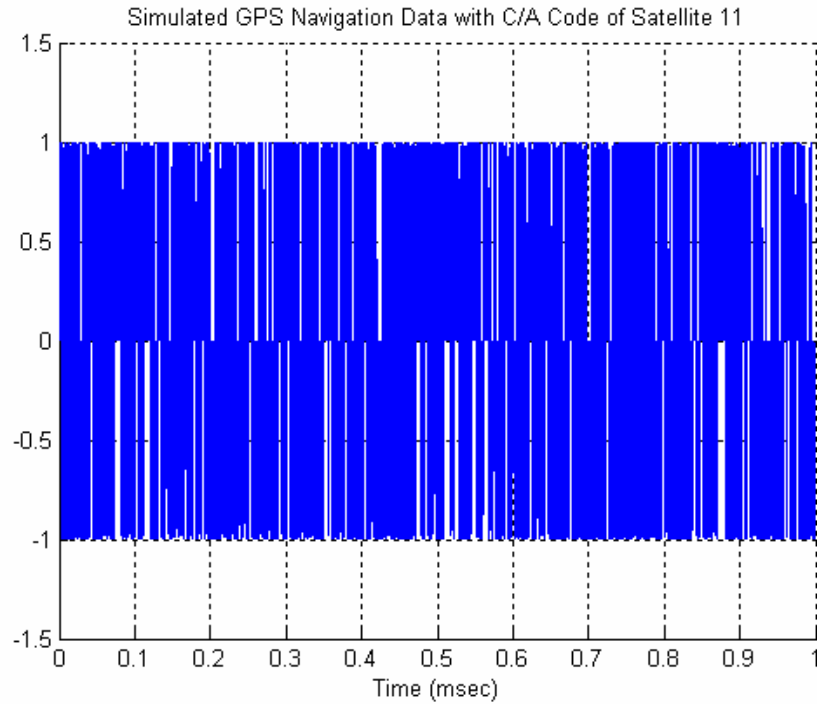


**Figure 3.6 Simulated Baseband GPS C/A Coded Data for Satellite 11**

For the convenience of testing purposes, the GPS signal is simulated at the IF carrier frequency of the Mitel GP2021 board. The simulated carrier has a frequency of 4.3097 MHz, chosen arbitrarily within the range of output IF frequency of the Mitel 2021 board. The power spectrum of the carrier is presented in Figure 3.7.

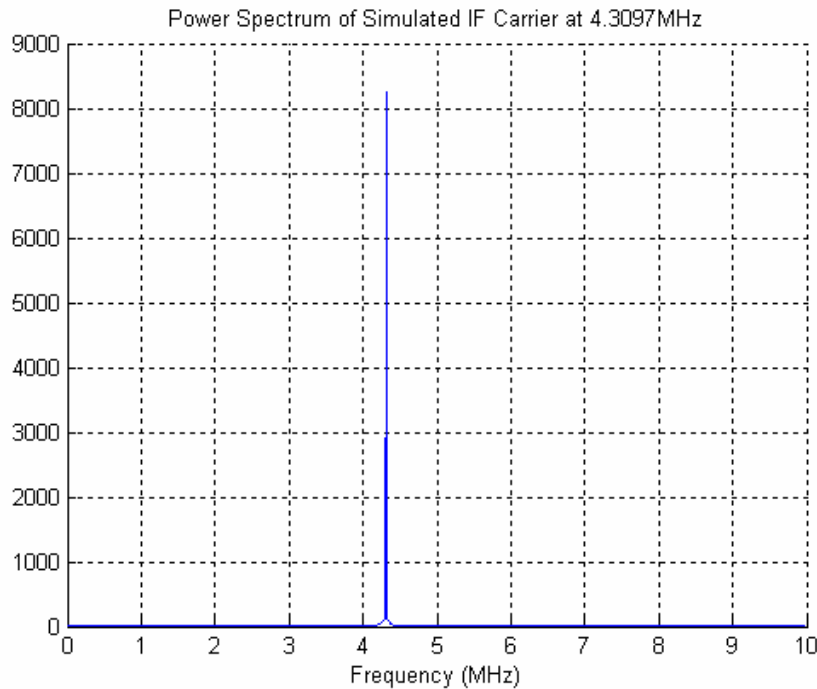


**Figure 3.7 Power Spectrum of Simulated IF Signal**

The final MATLAB simulated GPS signal contains no noise or Doppler shift. The power spectrum of the signal for one millisecond is shown in Figure 3.8. The simulated GPS signal is plotted in the time domain in Figure 3.9 a. A detailed view of the BPSK signal is shown in Figure 3.9 b. It can be seen that the phase is discontinuous whenever there is a bit transition. Since the IF carrier is at 4.3097 MHz, the waveform in Figure 3.9 b contains approximately 4 cycles in each microsecond, which corresponds to the intermediate frequency.

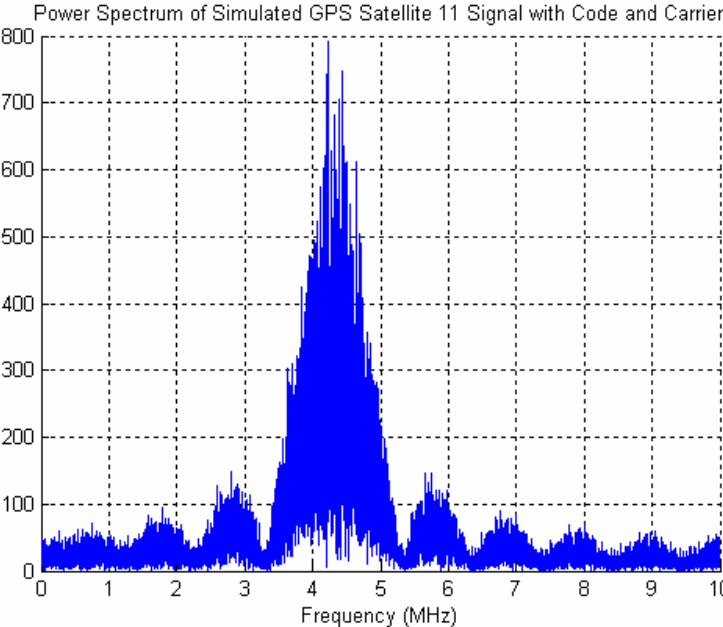


**Figure 3.8 Spectrum of Simulated GPS C/A Coded Data for Satellite 11 at IF**

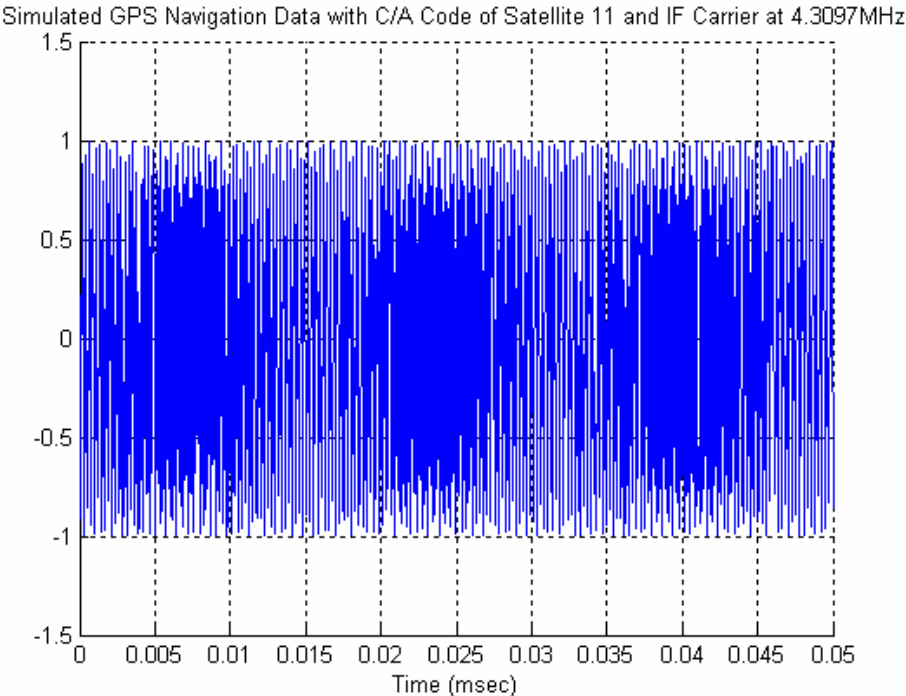


**Figure 3.9 a Simulated Baseband GPS C/A Coded Data for Satellite 11 at IF**

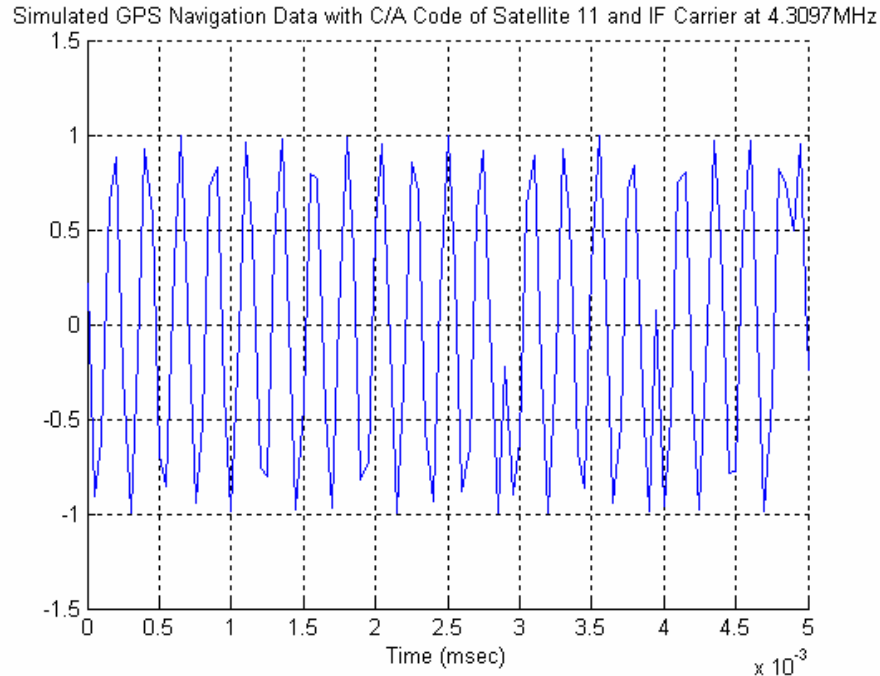


**Figure 3.9 b Simulated Baseband GPS C/A Coded Data for Satellite 11 at IF (Close-up)**

### 3.3.2 RF Signal from GSS 6560 Signal Simulator

Other than the simple version of the MATLAB simulated GPS signal, more realistic and longer GPS input data is needed to test the software receiver. To ensure the quality of the input signal, a simulator is used to create RF signals used as the input to the front-end of the software GPS receiver. The Spirent GSS 6560 Multichannel GPS/SBAS simulator employs an all-digital modulation scheme that produces a simulated GPS signal of very high resolution. The Spirent GSS 6560 GPS/SBAS simulation system with SimGEN provides a complete simulated RF environment that produces GPS L1 C/A code signals. The GSS 6560 simulator can simulate up to 12 channels of L1 frequency C/A coded GPS signals. It generates the GPS signals through the control of the SimGEN software over a USB link. The simulated output RF signals take account of the effects of high-dynamic vehicle motion, navigation satellite motion. Also the delays caused by Ionosphere and Troposphere on the signal are simulated using built-in Ionosphere and Troposphere models.

The GSS 6560 simulator comprises of two primary elements. The first element is multi-channel RF signal generator. Each generator provides the actual signals that stimulate the receiver or sensor, which channel represents a satellite signal at a single carrier frequency. Each channel can simulate either a direct satellite signal or a multipath signal. Figure 3.10 shows two GSS 6560 and an STR 4500 simulators stacked together. These two GSS6560 simulators in the GPS lab are capable of simulating two independent vehicles simultaneously. The STR 4500 simulator at the top is an older simulator that also produces up to 12 channels of C/A coded RF signals at L1 frequency.



**Figure 3.10 GPS Simulators Hardware Setup**

The second element is the SimGEN software which allows the specification, development and execution of simulations. The simulation takes the form of a scenario defined via a set of description or source files, each of which has its own specific editor. During the actual simulation, SimGEN runs models that act on the source file information and calculate the pseudorange between the simulated visible satellites and the simulated vehicle in which the receiver is installed [4]. Figure 3.11 gives a screen shot of the SimGEN scenario used to generate the input signal to the software receiver.



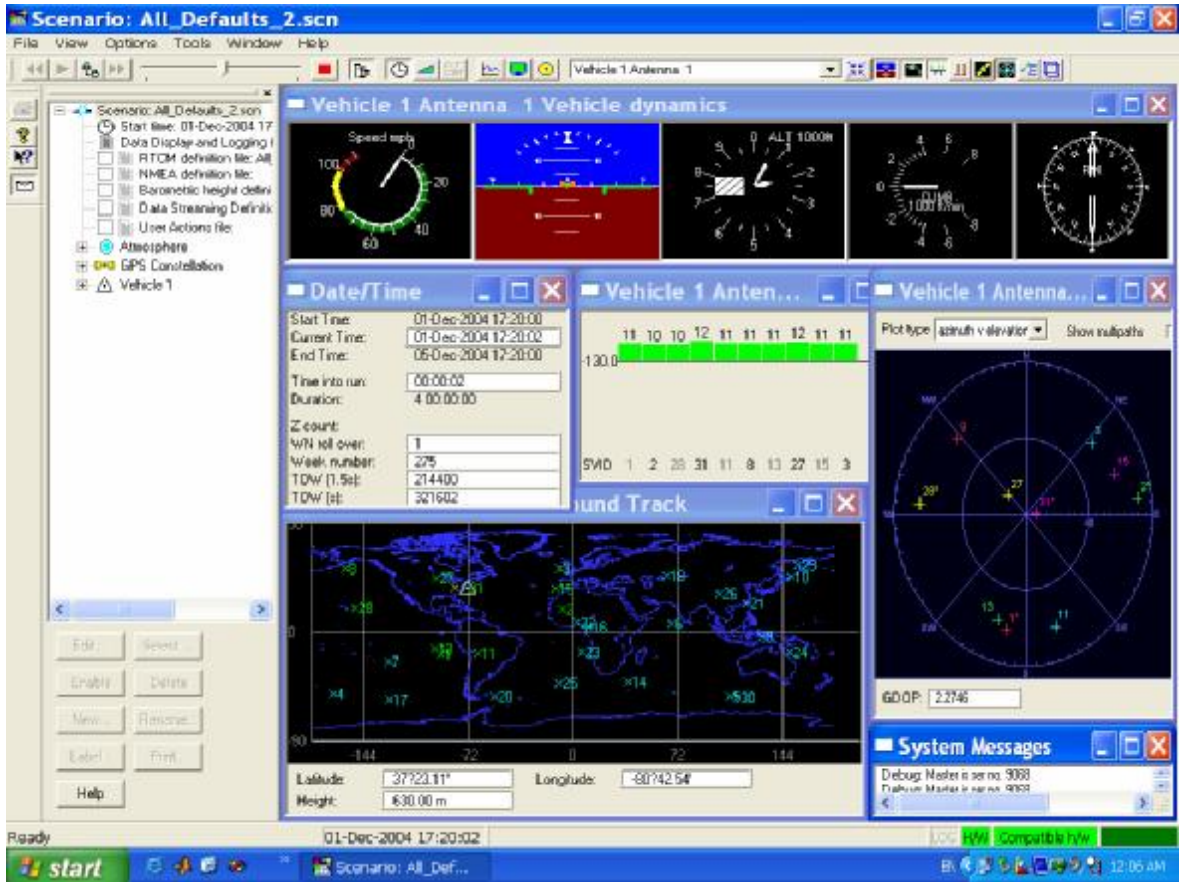


Figure 3.11 Screen Shot of SimGEN Scenario

The simulated data is used to test the acquisition and tracking programs initially because it does not contain noise or Doppler shift. After this verification of the program, the GPS signal from the GSS 6560 simulator will be used to evaluate the performance of the acquisition and tracking processes.

## CHAPTER 4 GPS C/A CODE SIGNAL ACQUISITION

The GPS signal from the simulator is a combination of carrier wave, C/A code and navigation message. In order to extract the navigation data from the GPS signal, it is necessary to remove the carrier wave and the C/A code. The process of receiving GPS signals may be divided into three steps: acquisition, tracking, computing the position solution from recovered navigation data bits. Acquisition is used to detect the presence of a signal from a particular satellite and calculate the initial code offset and Doppler shifted carrier frequency. The tracking process, bit synchronization, and sub-frame synchronization are used to keep lock on the carrier and code and to obtain pseudorange, carrier phase measurements from the recovered navigation data bits. In a conventional receiver, the front-end, the acquisition and tracking processes, are implemented in hardware while the navigation solution calculations are completed in software. This thesis focuses on the acquisition and tracking of the signals through software implementations

The two most important parameters to be determined by the acquisition program are the beginning of the C/A code and the carrier frequency of the input signal. The typical received signal contains information from more than one GPS satellite. For each satellite, the beginning of the C/A code and the carrier frequency after Doppler shift are different from others. Once the acquisition program detects the presence of a desired satellite and finds the beginning of the C/A code, it uses the information to despread the signal. After the despread of the spectrum, the signal becomes a continuous carrier wave. The carrier frequency of the signal can then be determined. The estimated beginning of the C/A code and the carrier frequency are then passed onto the tracking program [1].

The beginning of the C/A code and the IF carrier frequency of a GPS signal from a satellite can be found by correlating the incoming signal with the receiver generated signal. There are several different methods to perform acquisition. The two methods analyzed are the serial search in time domain and parallel search using fast Fourier transform (FFT) in frequency domain. Though serial search is the slowest search method, it is usually implemented in hardware based receivers due to its simplicity. The parallel search (FFT method) in frequency domain usually implemented by software receiver since serial search method is computation intensive in the software approach.

#### **4.1 Factors Affecting the Acquisition Performance**

Several factors can affect the performance of the acquisition program. One of the most important factors is the length of data used to acquire the code offset and Doppler shifted frequency. Another factor is the frequency search step in calculating the carrier frequency. More search steps will provide finer frequency at the cost of more processing time.

##### **4.1.1 Data Length for Acquisition**

It is important to determine the length of data necessary to perform acquisition. The longer the data the longer is the processing time. The benefit of using a longer period of data is the improvement of the SNR of the signal. However, if fast acquisition is critical for the implementation of software-based GPS receiver, the optimum length of data should be used for successful fast acquisition. The two factors that limit the selection of longer data period are the length of the navigation data and the change in Doppler frequency.

Since the navigation data length is 20 ms, if the first 10 ms of the data has a phase transition due to the navigation data bit, there will be no phase transition in the next 10 ms of data. Therefore, the maximum data length that can be used is 10 ms. Since the C/A code is one millisecond long, the beginning of a C/A coded input signal can be found within this amount of data. However, there is still the possibility that a phase transition due to the navigation data occurs in this one millisecond of data. If the transition occurs in this one millisecond of data, the next one millisecond of data cannot contain another navigation data bit transition. In order to guarantee that there is at least one set of data with no data bit transition, a minimum of two consecutive milliseconds of data should be used for successful acquisition. As noted previously, a maximum length of 10 ms of data can be ensured to contain no navigation data bit transition. There is a tradeoff between the processing time and data length used for acquisition. Only one or two milliseconds of data are required for strong signals while the weaker signals need five to ten milliseconds of data for acquisition [5]. However, the strength of a signal from a particular satellite is difficult to determine before

acquisition. Therefore, the acquisition program processes at least two consecutive data sets. The data length cannot exceed 10ms unless a technique to handle the navigation data transition effect during the acquisition process is implemented [6]. High sensitivity can be achieved using the tracking program.

The signal-to-noise ratio can be increased by processing longer periods of data in the acquisition process. However, the extended data will also increase the processing time. If a navigation data transition occurs in the input signal to be processed, the despread signal will no longer be a continuous carrier wave. Since there is at most one data bit transition in any 20 ms of the input signal, if a navigation data bit transition occurs in the first 10 ms of data, the next 10 ms of data will be continuous. In actual acquisition, even if there is a phase transition due to a navigation data bit, the spectrum spreading is not very wide [1]. The correlation peak usually can be detected, so the beginning of the C/A code can be found.

#### **4.1.2 Doppler Frequency Search Step**

Doppler frequency search step is another key factor for successful and fast acquisition. Since the carrier frequency is affected by the Doppler shift, the shift has to be accounted for in the receiver generated signal. However, the exact Doppler shift is unknown, so the search needs to cover the range of all possible Doppler frequencies. The maximum Doppler frequency that needs to be searched is  $\pm 10$  kHz which is the sum of both the Doppler on the C/A code and on the carrier[3]. However, the number of frequency steps necessary to cover the 20 kHz frequency range needs to be determined. Widening the bandwidth of the searching steps improves the speed of the search. Using a narrow bandwidth in the search process requires more steps to cover the same desired frequency range resulting in more computation time. However, searching with narrow bandwidth steps improves the sensitivity. The frequency step is related to the length of data used in acquisition [1]. From the correlation properties of the GPS C/A code signals, it can be seen that when the input signal and the locally generated complex signal are off by one chip, there is no correlation. If the two signals are off by less than one chip, there is partial correlation. When the two signals are misaligned by half a chip, the peak correlation amplitude decreases by 6dB [5]. To ensure there is still partial correlation between the input signal and the locally generated signal, the maximum frequency separation should be within half a chip. If the data length is 1 ms, 1 kHz signal will change one cycle in 1ms. In order to keep the maximum frequency separation within half a cycle in 1ms, the frequency step should be 1 kHz. Hence, the furthest frequency separation between the input signal and receiver generated signal is 500Hz. If the data length is 10ms, the search frequency step should be 100Hz.

Also visible satellites in the incoming signal are not necessarily known in advance, so the search needs to search for all possible satellites. Therefore, the receiver needs to generate signal at different carrier frequencies with different C/A codes. If the visible satellites are known, then the search range can be significantly limited and reducing the computation time.

## **4.2 Acquisition Methods**

The conventional approach to signal acquisition is to search for the satellites in the time domain through hardware. The search for the satellites can be performed in series as well as in parallel depending on the hardware design. In a software receiver, the acquisition is generally performed on a block of data using parallel search algorithm. After acquiring the

desired signal, the relevant parameters are then passed onto the tracking program. If the receiver is operating in real time, there will be a time lapse between the data used for acquisition and the data being tracked. If the acquisition program is slow in determining the beginning of the C/A code and the carrier frequency, the time gap between the acquisition and tracking programs will be more significant [3]. When the receiver does not process data in real-time, the speed of acquisition is not as important. However, in designing a real-time software receiver, an important consideration is the speed of signal acquisition.

#### 4.2.1 Serial Search in the Time Domain

Serial search is the simplest and most frequently used acquisition method especially in hardware GPS receivers. In a serial search, each possible frequency and code offset is evaluated serially until the correct values are found (when the value crosses a certain threshold). In this approach, the digital IF signal,  $x[n]$  is multiplied by the locally generated C/A code,  $CA[n+m]$  where  $n$  is the  $n$ -th sample and  $m$  is the number of phase shifted samples of the replicated C/A. Since the sampling rate is 20 MHz, the length,  $L$ , of one C/A code period is 20,000 samples nominally.

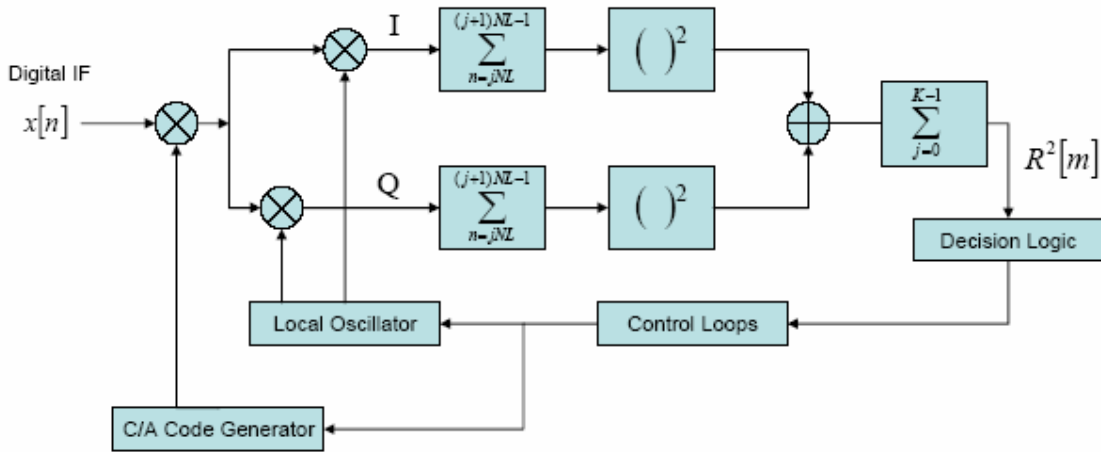


Figure 4.1 Algorithm for Serial Search Acquisition

After the C/A code is despread, the in-phase ( $I$ ) and quadrature ( $Q$ ) channels are generated after mixing with the local oscillator. The  $I$  and  $Q$  components are accumulated over  $N$  code periods, and the accumulated sum of these two channels is squared. The next  $K$  correlations are accumulated to produce an averaged correlation value. If the average correlation peak value crosses a certain threshold value, then the satellite is acquired. The correlation in discrete time domain is expressed as

$$R^2[m] = \sum_{j=0}^{K-1} \left( \left[ \sum_{n=jNL}^{(j+1)NL-1} x[n] \cdot CA[n] \cdot \cos[w \cdot n] \right]^2 + \left[ \sum_{n=jNL}^{(j+1)NL-1} x[n] \cdot CA[n] \cdot \sin[w \cdot n] \right]^2 \right) \quad \text{Eq. 4.1}$$

where  $\omega$  is the radian frequency. Setting  $N$  and  $K$  to smaller values allows faster acquisition. However, choosing larger values for  $N$  and  $K$  will improve the acquisition of weaker signals and reduce the probability of false acquisition [7]. Choosing a larger  $N$  value increases the possibility of a data bit transition in the correlation process, but it also improves the signal-to-noise ratio (SNR). The data transitions are synchronized to the code periods and occur only once every 20 code periods.

Usually when serial search is performed the code phase is incremented  $\frac{1}{2}$  chip when one code phase has been tested. Therefore, there are  $2 \times 1023 = 2046$  code phases that must be searched [6]. In the software receiver implementation, with the input signal sampled at 20 MHz, 40,000 samples of the received data are correlated with the locally generated C/A code by sliding the replicated code over the 40,000 samples. Figure 4.2 illustrates the linear search over the range of possible carrier frequencies. If there is some a priori information about either the carrier or code phase distribution, it is possible to use other more efficient serial search methods than the linear search algorithm. Linear search simply increments in the code phase and Doppler frequency linearly [7].

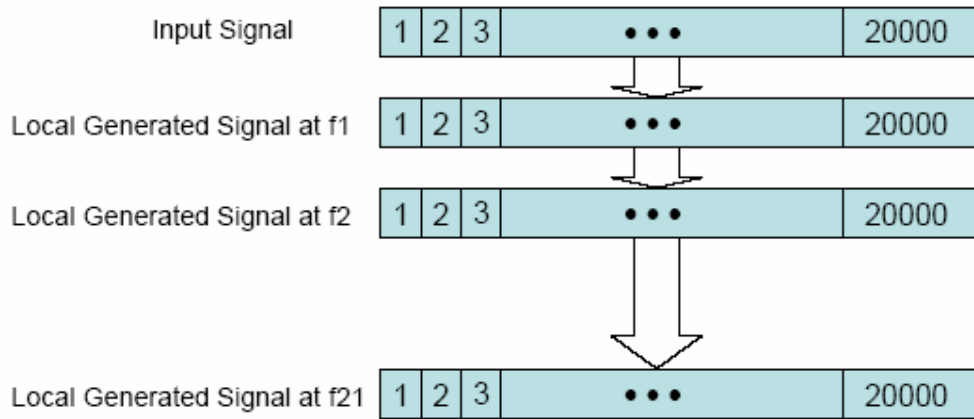


Figure 4.2 Linear Search Algorithm

#### 4.2.2 Parallel Search in the Frequency Domain using FFT

The output of a linear, time-invariant (LTI) system,  $y(t)$  can be found through convolution in the time domain and Fourier Transform in the frequency domain. The time domain convolution can be expressed as

$$y(t) = \int_{-\infty}^{\infty} x(t-t)h(t)dt = \int_{-\infty}^{\infty} x(t)h(t-t)dt \quad \text{Eq. 4.2}$$

where  $x(t)$  is the input signal and  $h(t)$  is the impulse response [1]. The corresponding frequency response  $Y(f)$  through the Fourier Transform is

$$Y(f) = \int_{-\infty}^{\infty} \int_{-\infty}^{\infty} x(t)h(t-t)dt e^{-j2\pi f t} dt = \int_{-\infty}^{\infty} x(t) \left( \int_{-\infty}^{\infty} h(t-t) e^{-j2\pi f t} dt \right) dt \quad \text{Eq. 4.3}$$

$$Y(f) = H(f) \int_{-\infty}^{\infty} x(t) e^{-j2\pi f t} dt = H(f)X(f)$$

where  $X(f)$  and  $H(f)$  are the Fourier Transforms of the input signal and the impulse response respectively. The output  $y(t)$  in the time domain is obtained from the inverse Fourier Transform.

$$y(t) = x(t) * h(t) = F^{-1}\{X(f)H(f)\} \quad \text{Eq. 4.4}$$

In discrete time concepts, the relationship in Eq. 4.4 can be expressed in terms of summations.

$$y(n) = \sum_{m=0}^{N-1} x(m)h(n-m) \quad \text{Eq. 4.5}$$

where  $x(m)$  is the input signal and  $h(n-m)$  is the impulse response in discrete time domain. The discrete Fourier Transform (DFT) of the output is

$$\begin{aligned} Y(k) &= \sum_{n=0}^{N-1} \sum_{m=0}^{N-1} x(m)h(n-m)e^{-\frac{j2\pi \cdot k \cdot n}{N}} \\ Y(k) &= \sum_{n=0}^{N-1} x(m) \left[ \sum_{m=0}^{N-1} h(n-m)e^{-\frac{j2\pi \cdot (n-m)k}{N}} \right] e^{-\frac{j2\pi \cdot m \cdot k}{N}} \quad \text{Eq. 4.6} \\ Y(k) &= H(k) \sum_{n=0}^{N-1} x(m)e^{-\frac{j2\pi \cdot m \cdot k}{N}} = X(k)H(k) \end{aligned}$$

This is circular convolution, which is different from linear convolution. In linear convolution, if the input and the impulse response of the system both contain  $N$  points of data, the system output has  $2N-1$  points. However, in circular convolution, the output is only  $N$  points. This is due to the periodic nature of the DFT [1].

In the acquisition process, correlation, rather than convolution is used. The correlation between  $x(n)$  and  $h(n)$  can be expressed as

$$z(n) = \sum_{m=0}^{N-1} x(m)h(n+m) \quad \text{Eq. 4.7}$$

In the case of correlation,  $h(n)$  is not the impulse response of the system, but that of another signal. The DFT of  $z(n)$  is

$$\begin{aligned} Z(k) &= \sum_{n=0}^{N-1} \sum_{m=0}^{N-1} x(m)h(n+m)e^{-\frac{j2\pi \cdot k \cdot n}{N}} \\ Z(k) &= \sum_{n=0}^{N-1} x(m) \left[ \sum_{m=0}^{N-1} h(n+m)e^{-\frac{j2\pi \cdot (n+m)k}{N}} \right] e^{\frac{j2\pi \cdot m \cdot k}{N}} \quad \text{Eq. 4.8} \\ Z(k) &= H(k) \sum_{n=0}^{N-1} x(m)e^{\frac{j2\pi \cdot m \cdot k}{N}} = H(k)X^{-1}(k) \end{aligned}$$

where  $X^{-1}(k)$  is the inverse DFT. The magnitude of  $Z(k)$  can be written as

$$|Z(k)| = |H^*(k)X(k)| = |H(k)X^*(k)| \quad \text{Eq. 4.9}$$

The parallel search algorithm can also be implemented using circular correlation. The 20,000 samples of the received data are correlated with the replica code by circularly shifting the replica code. The circular correlation is a multiplication in the frequency domain that can be expressed as.

$$R[m] = x[n] \otimes CA[-n] = F^{-1}(F(x[n]) \cdot F(CA[n])^*) \quad \text{Eq. 4.10}$$

*Circular Correlation*

where the fast Fourier transform (FFT) and its inverse (IFFT) is used to calculate  $R$  [7]. Since the fast Fourier transform is used to implement the DFT and IDFT, the acquisition is also called the FFT search. In the case of the software GPS receiver, the incoming signal is mixed to baseband and the in-phase and quadrature components are used as the real and imaginary inputs when calculating the FFT. The result is multiplied by the complex conjugate of the FFT of the C/A code. The circular correlation is obtained by taking the magnitude of the inverse FFT of the result. Figure 4.3 presents the implementation of the parallel search in the frequency domain.

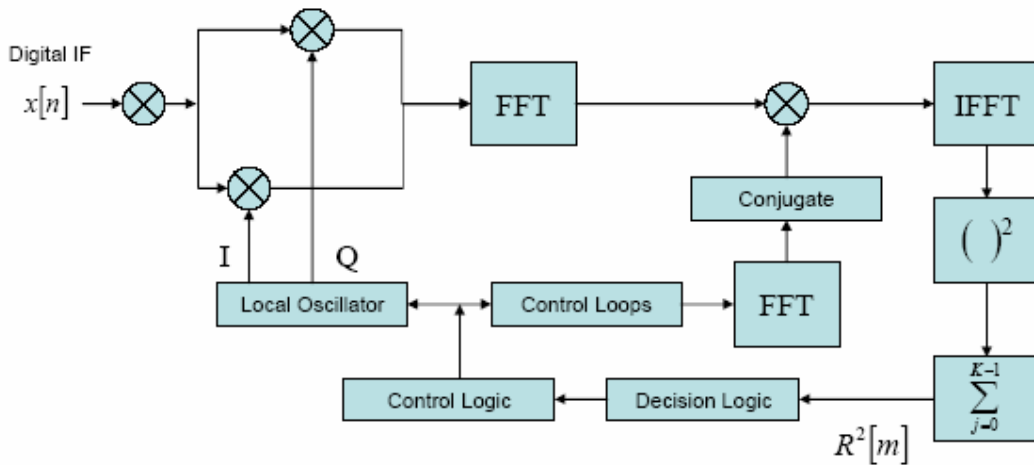


**Figure 4.3 Algorithm for Parallel Search FFT-based Method Acquisition**

The acquisition program of the software receiver uses the circular correlation method to find the signal. Only 1ms of input data is used to obtain the beginning of the C/A code initially. Since the sampling frequency of the signal is 20 MHz, there are 20,000 samples in one C/A code period of duration one millisecond. Since the C/A code does not necessarily start at the beginning of the input data, the beginning of the C/A code needs to be found before despreading the data. A local copy of the specific C/A code is generated for 1 ms and digitized at a frequency of 20 MHz to create the 20,000 samples needed. The digitized code is then slid over the 20,000 sample input data to find the peak correlation value.

If the digitized C/A code with the correct phase is multiplied with the input signal, the input signal will be a continuous carrier wave. Once the signal becomes a carrier wave, the frequency of the signal can be determined through an FFT operation [1]. If the input data length is 1 ms long, the FFT will have a frequency resolution of 1 kHz. A threshold needs to be set to determine if the frequency component is strong enough. The highest frequency above the threshold is the desired frequency component [1].

Since the signal is digitized at 20 MHz, 1 ms of data contains 20,000 data points, so a 20,000-point FFT contains 20,000 frequency components. However, only the first 10,000 points of the FFT contains useful information. The second half of the frequency components is the complex conjugate of the first half [1]. Since the frequency resolution is 1 kHz, the total frequency range covered by the FFT is 10 MHz, which is half of the sampling frequency. . If a 20,000 point FFT is performed on each of the 20,000 multiplications, a total of 20,000 frames of data each containing 10,000 useful frequency components is produced. There are a total of  $2.0 \times 10^8$  outputs in the frequency domain. Assuming the threshold is crossed, the highest amplitude of these outputs contains the desired information about the carrier frequency and the beginning of the C/A code [1]. However, searching and comparing all  $2.0 \times 10^8$  frequency components is computational intensive and time consuming. Since the interested frequency range is only  $\pm 10$  kHz of the ideal carrier frequency taking account of the Doppler shift, the acquisition program generates carrier waves for a frequency range of  $\pm 10$  kHz from the ideal carrier frequency with a frequency step of 1000 Hz. With the 1 kHz frequency step, a total of 21 Doppler frequency steps can cover the desired search range of  $\pm 10$  kHz from the center frequency. Searching only the 21 frequency components can significantly reduce the computation time. Performing FFT on 20,000 points with 21 frequency components will generate altogether 420,000 ( $20,000 \times 21$ ) point outputs. This signal is correlated with receiver generated C/A code and carrier frequency with Doppler frequency range of  $\pm 10$  kHz at steps of 1 kHz. The frequency resolution of the acquisition program is 1 kHz. The beginning of the C/A code has a time resolution of 50ns ( $1/20\text{MHz}$ ).

If 10 ms of data is used, the signal only needs to be correlated for 1 ms because the length of the C/A code is only 1 ms. Each operation consists of a 20,000-point multiplication and a 200,000-point FFT. The total number of useful output is  $2.0 \times 10^9$  ( $20,000 \times 100,000$ ). By lengthening the input data used for acquisition, the operation time increases significantly. Though the time resolution of the beginning of the C/A code remains 50 ns, the frequency resolution improves by a factor of 10 to 100 Hz.

#### 4.2.3 Fine Carrier Frequency Resolution

To find the carrier frequency with finer resolution, the FFT is no longer an efficient method. To obtain 10 Hz frequency resolution with FFT, the data length required is 100 ms. With the sampling rate of 20 MHz, a total of 2,000,000  $\left(20,000,000 \times \frac{100}{1000}\right)$  points FFT has to be computed, which is a time consuming operation. The final estimated carrier frequency is calculated using its phase relationship. The initial carrier frequency is estimated to be the highest frequency component of the FFT. Let the highest frequency at time  $m$  be represented as  $X_m(k)$ , where  $k$  is the  $k$ -th frequency component calculated in the FFT. The initial phase  $q_m(k)$  can be calculated using the real and imaginary components of  $X_m(k)$  as

$$q_m(k) = \tan^{-1} \left( \frac{\text{Im}(X_m(k))}{\text{Re}(X_m(k))} \right) \quad \text{Eq. 4.11}$$

A second estimate of the phase can be found at time  $n$ , some time after the occurrence of  $m$ . The phase at time  $n$  of frequency component  $k$ ,  $q_n(k)$  can be calculated as



$$q_n(k) = \tan^{-1} \left( \frac{\text{Im}(X_n(k))}{\text{Re}(X_n(k))} \right) \quad \text{Eq. 4.12}$$

The fine frequency estimate can be calculated with the phase change between time  $m$  and  $n$  as

$$f = \frac{q_n(k) - q_m(k)}{2p(n-m)} \quad \text{Eq. 4.13}$$

In order to keep the frequency unambiguous, the phase difference  $q_n(k) - q_m(k)$  must be less than  $2p$ . If the phase difference is at the maximum value of  $2p$ , the unambiguous bandwidth is  $\frac{1}{(n-m)}$ , where  $(n-m)$  is the delay time between two consecutive sets of data [1].

Initially, the FFT of each millisecond of data is computed with the frequency resolution of 1 kHz. If the actual carrier frequency of the input signal is between two frequency components, there will be uncertainty in the phase. To eliminate this ambiguity, the amplitude comparison technique is implemented. Let the amplitude of the highest frequency component  $k$  of the FFT be  $X(k)$ , the two adjacent frequency components have amplitudes  $X(k-1)$  and  $X(k+1)$ . The amplitudes of  $X(k-1)$  and  $X(k+1)$  are compared to find the stronger of the two. If the amplitude of  $X(k-1)$  is higher, then the actual carrier frequency is lower than the frequency of  $X(k)$ , otherwise it is higher than that of  $X(k)$ .

If there is a navigation data bit transition between two consecutive sets of data, a phase shift of  $p$  is introduced. In this case, the input signal no longer has a continuous phase. If this phase transition is not accounted for, the estimated frequency will be off by  $p$  which corresponds to a 500 Hz frequency offset with 1 kHz frequency resolution. To avoid this source of error, the unambiguous bandwidth is limited to 250 Hz. To account for the effect of noise, the maximum frequency uncertainty allowed is reduced to  $\pm 200$  Hz which

corresponds to a phase angle difference of  $\pm \frac{2p}{5}$ . With this maximum allowed frequency

offset, a phase transition caused by the navigation data bit will cause an offset of  $\pm \frac{3p}{5}$

or  $\pm \frac{7p}{5}$ . The magnitudes of both offset values are outside the maximum allowed frequency

offset range. When a frequency offset outside the maximum allowed range occurs,  $p$  is either added or subtracted from the frequency offset to account for the navigation data bit transition. Therefore, the calculated frequency is kept to within 200 Hz of the ideal frequency component value. The maximum frequency offset between two adjacent  $k$  values in  $X(k)$  is kept to 400 Hz.

In the acquisition program, the FFT of one millisecond of data is first calculated as  $X(k)$ . The complex conjugate of  $X(k)$  is computed and denoted as  $X^*(k)$ . Since the Doppler shift range covers 21 frequency components with 1 kHz frequency resolution, a local code  $c_i(n)$  ( $i = 1, 2, \dots, 21$ ), is generated for each of these frequency components. The locally generated

codes are also sampled at 20 MHz, where  $n$  denotes the sample numbered  $1 \dots 20,000$ . The FFT of the digitized local codes are then computed as  $C_i(n)$ . To remove the C/A code from the incoming signal, the FFT of the input data is multiplied with the FFT of each of the locally generated codes. The inverse FFT of their products are found in the time domain. The absolute maximum of the result contains the frequency resolution in 1 kHz and the beginning of the C/A code in 50 ns resolution. To find the carrier frequency to 200 Hz resolution, two DFT operations are performed on the same set of data. One DFT is calculated at a frequency 400 Hz lower than the highest frequency component and another 400 Hz higher. The amplitudes of the three DFTs are compared and the frequency of the highest component is set as the new carrier frequency. The new frequency is within 200 Hz of the true carrier frequency. The locally generated code is then multiplied with the next 5 ms of data to remove the C/A code. The remaining signal only contains the navigation data bits. The highest frequency component for each of the 5 ms are calculated as  $X_n(k)$  where  $n = 1, 2, \dots, 5$ . The difference in the phase angle between two consecutive sets of data is defined as  $\Delta q = q_{n+1} - q_n$ . In this case, the final fine frequency is the average of the four sets of frequencies.

### 4.3 Performance of the Acquisition Program

To verify that the acquisition program works properly, the simulated data (described in section 3.4) was first used as the input signal. Figure 4.4 illustrates the result of the acquisition process for simulated GPS signal of satellite 11. The peak is where the estimated carrier frequency and beginning of the C/A code for satellite 11 as calculated by the acquisition program.

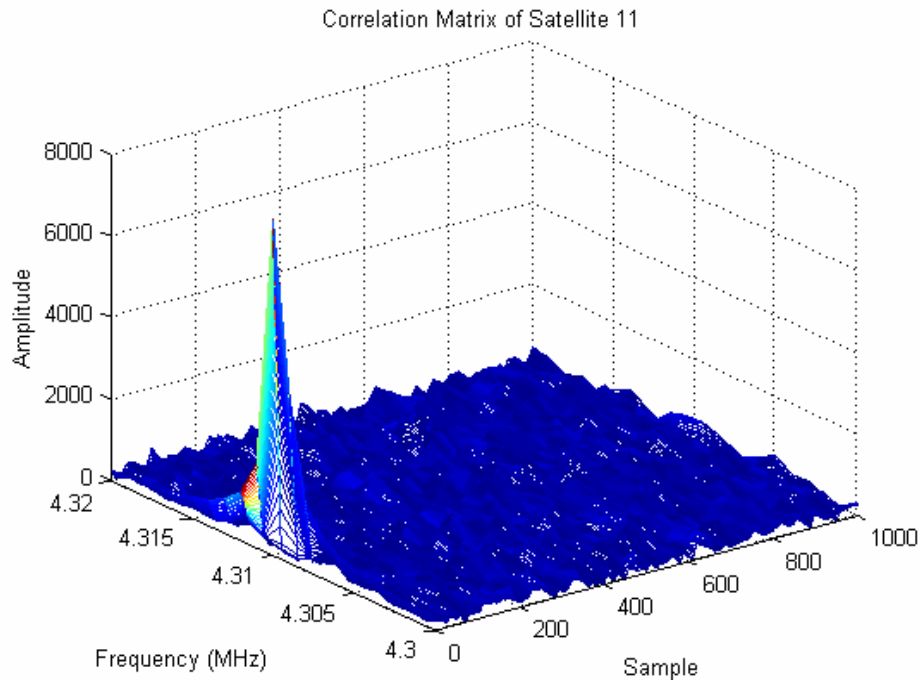


**Figure 4.4 Acquisition of Satellite 11 at IF 4.3097 MHz**

There was no phase shift or C/A code offset added in the simulation, so the resulting signal should have a carrier frequency that matches the original carrier frequency and the

beginning of the C/A code should be at 1. Figure 4.5 and 4.6 breaks the plot in Figure 4.4 into two different 2-D components. From Figure 4.5, it can be seen that the acquisition program found the beginning of the C/A code of satellite 11 to be at sample one. In Figure 4.6, the carrier frequency returned by the acquisition program is 4.3097 MHz. The true carrier frequency of the simulated signal is 4.3097 MHz. In this case, the carrier frequency returned by the acquisition program matches that of the simulated signal.

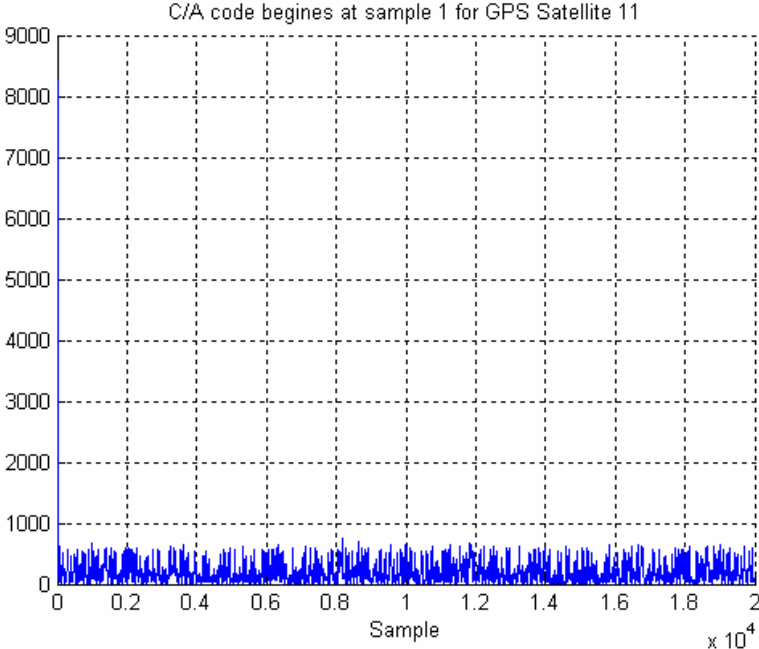


**Figure 4.5 The Correlation Output of Input Signal and the C/A Code of Satellite 15**

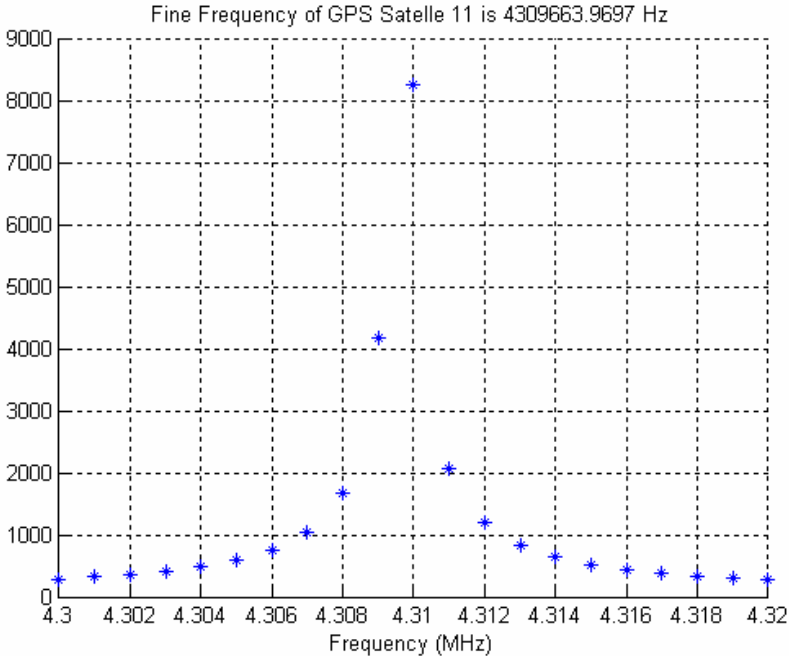


**Figure 4.6 Frequency Component of the Despread Signal of Satellite 15**

Once the acquisition program is verified to work with the simulated GPS signal, the GPS signal from the GSS 6560 simulator is used as the new input signal. The digitized input

signal is shown in Figure 4.7 a. A more detailed view of the input signal can be found in Figure 4.7 b. Since the signal is extracted from a pin on the Mitel 2021 board, the signal strength is much weaker compared to the simulated signal using MATLAB.

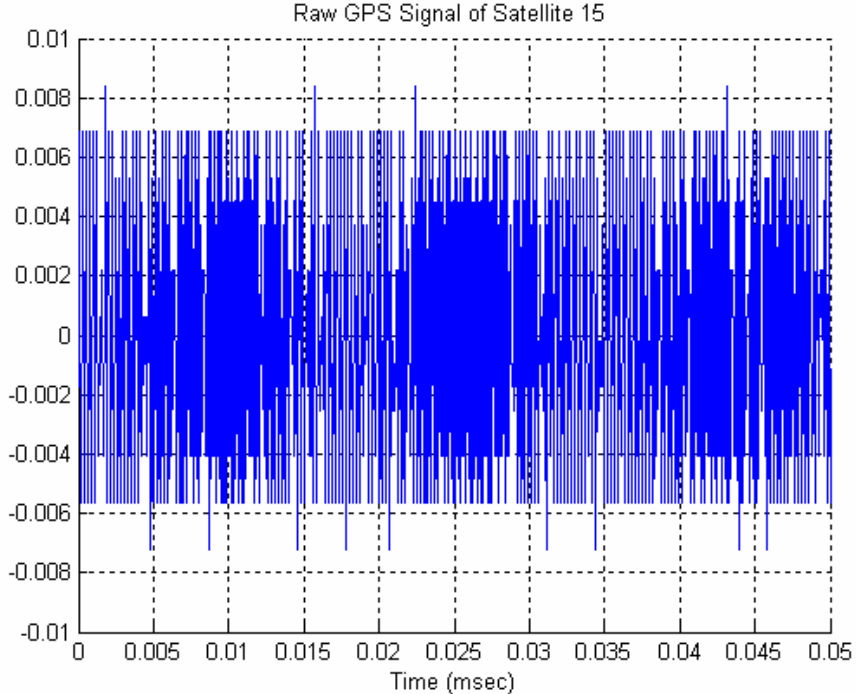


Figure 4.7 a Raw GPS Input Signal from Satellite 15 at IF

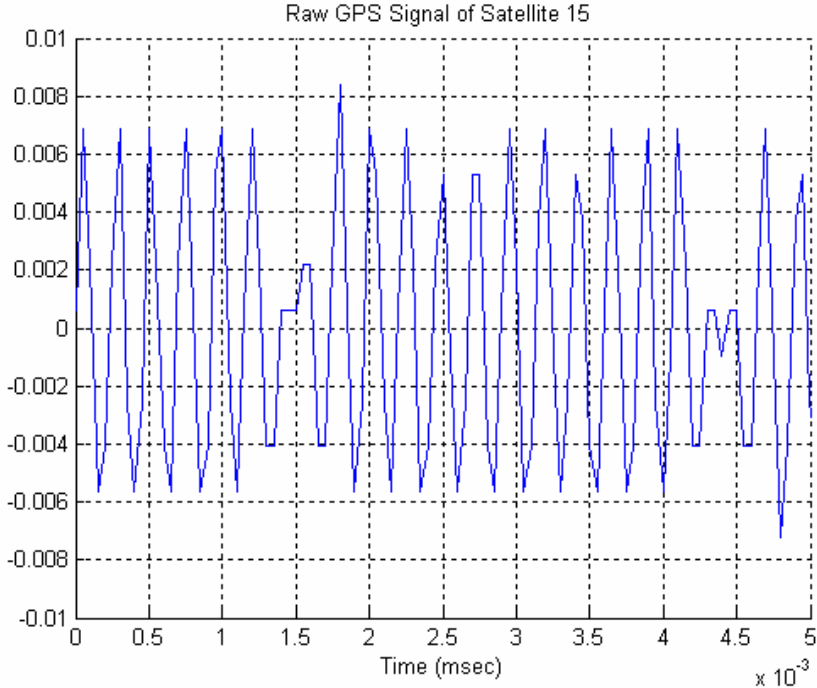
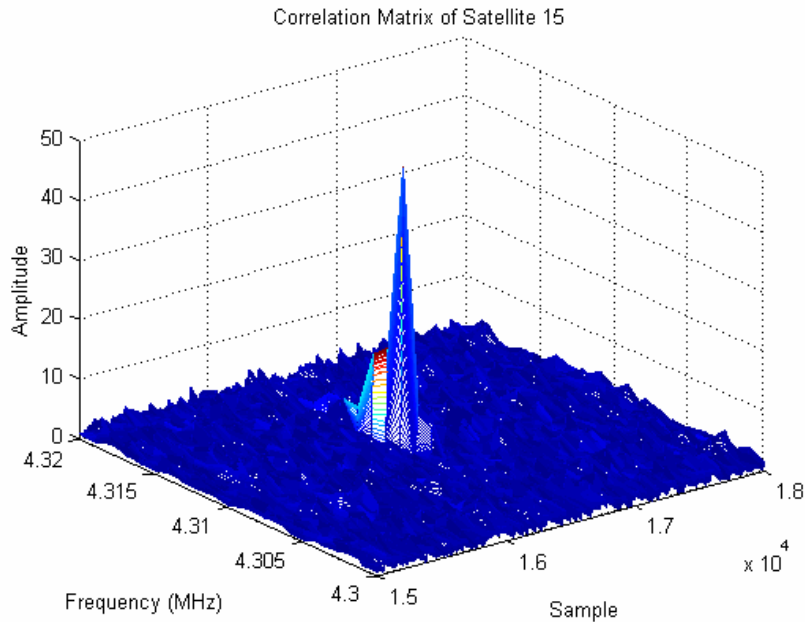


Figure 4.7 b Raw GPS Input Signal from Satellite 15 at IF (Close-up)

The correlation matrix for the signal from satellite 15 is illustrated in Figure 4.8. Again, the acquisition program returns the calculated position of the beginning of the C/A code and estimated carrier frequency.



**Figure 4.8 Acquisition of Satellite 15 at IF 4.31 MHz**

For this particular set of data collected from satellite 15, the outputs of the acquisition program is shown in Figures 4.9 and 4.10. In the 20,000 point sampled input data of 1ms, the beginning of the C/A code is calculated to be at sample 16355. The correlation peak at this sample value is much greater than the cross-correlation values. This result further verifies the correlation property of the C/A codes. The highest frequency component shown in Figure 4.6 is the estimated carrier frequency with the Doppler shift.

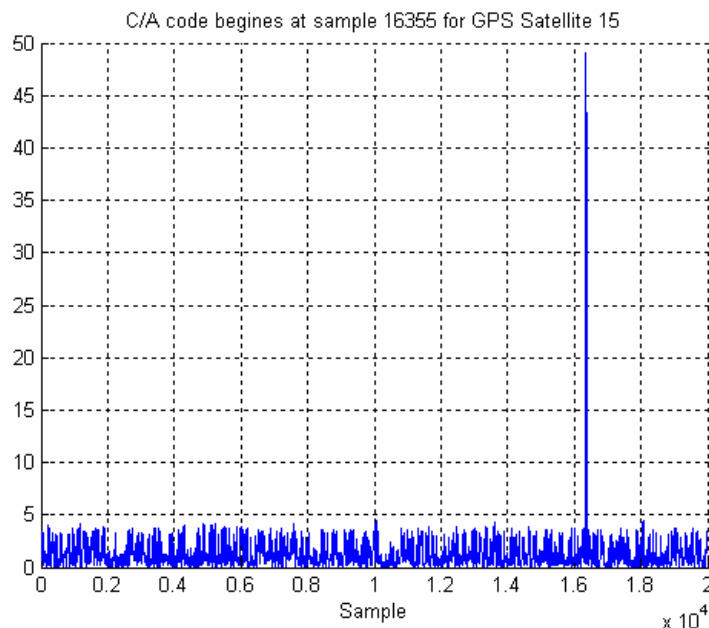


**Figure 4.9 The Correlation Output of Input Signal and the C/A Code of Satellite 15**

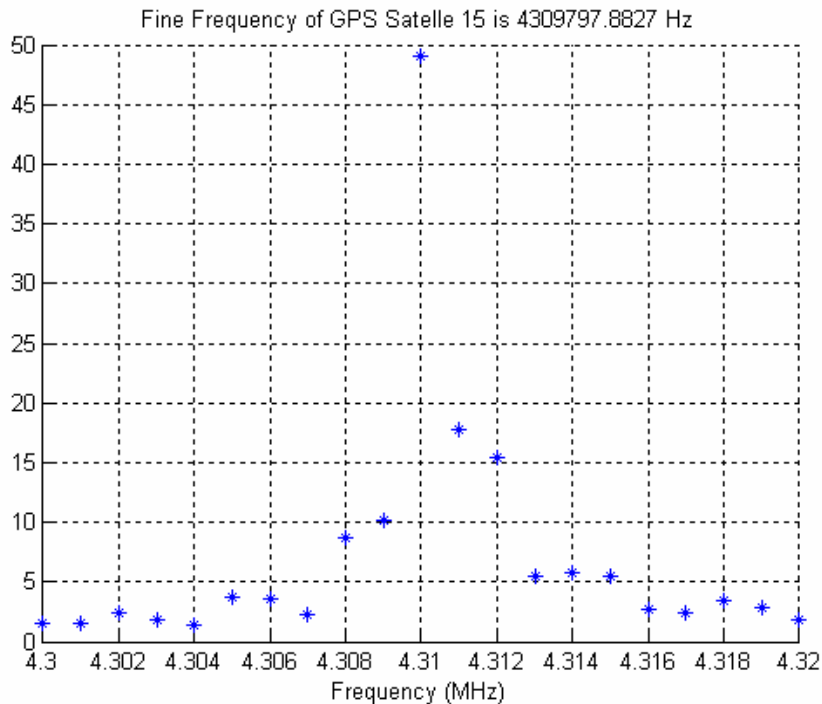


**Figure 4.10 Frequency Component of the Despread Signal of Satellite 15**

From the results, it can be verified that the Doppler shift did not cause the ideal carrier frequency to shift much. The initial estimated carrier frequency is still 4.31 MHz. However, the final carrier frequency output of the acquisition program is 4.309797 MHz. This value is obtained after several frequency refined searches. Since the initial frequency resolution is 1 kHz, the estimated carrier frequency will be too coarse for the tracking program. The bandwidths of the tracking loops are very narrow, so the final estimated carrier frequency should be within a few Hertz of the actual carrier frequency.

The acquisition search returns the frequency and phase of the PRN code for a specific satellite. If the user is moving at a considerable speed and is frequently changing direction the receiver may lose the satellite signal. If the frequency deviations are not corrected for, the receiver will eventually lose track of the satellite and no data will be decoded. The outputs of acquisition are used for tracking the signal so that both carrier and code can be stripped off from the incoming signal.

## CHAPTER 5 TRACKING OF GPS C/A CODE SIGNAL

After the acquisition process is complete, the receiver enters the tracking phase. A delay-locked loop (DLL) is used to track the C/A code phase and a phase-locked loop (PLL) is used to track the carrier frequency of the incoming signal with Doppler shift. When both tracking loops are in lock, it is possible to decode the 50 Hz navigation data message. The tracking loop follows the incoming signal and adjusts itself to de-spread and de-modulate the incoming signal. If the receiver is stationary, the rate of change of Doppler frequency is small so the update rate of tracking loop is less frequent.

## 5.1 Code Tracking

Since the phase of the incoming GPS signal is not constant, the code tracking process becomes necessary to remove the phase shift in the C/A code such as the effect of noise. When a phase shift occurs, the correlation peak of the locally generated code and the incoming signal will decrease. However, only knowing that a phase shift has occurred is not sufficient, the direction of the shift needs to be determined in order to compensate its effect.

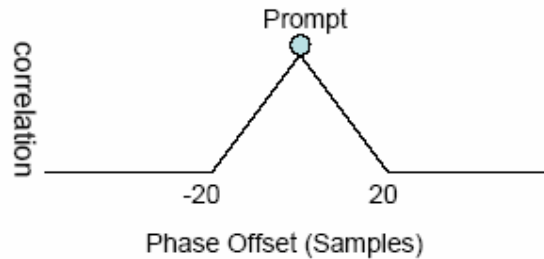


Figure 5.1 Ideal Correlation of C/A Code and Input Signal

### 5.1.1 The Early, Prompt and Late Codes

Ideally, the correlation between the local C/A code and the input signal decreases linearly from its peak correlation value to zero at 20 samples when the phase shift between the two signals reaches one full chip. From the properties of the orthogonal codes, there should be no correlation when two signals are misaligned by a chip or more. Therefore, the cross-correlation between different PRN codes is treated as noise. When a phase shift occurs, the peak correlation value will either slide to the left or the right of the ideal correlation curve.

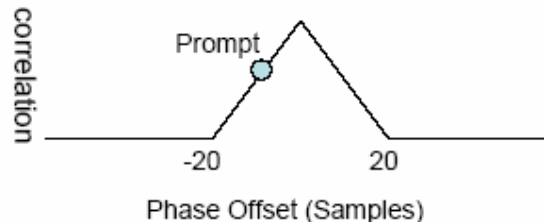


Figure 5.2 Correlation of C/A Code and an Input Signal with Phase Shift to the Left

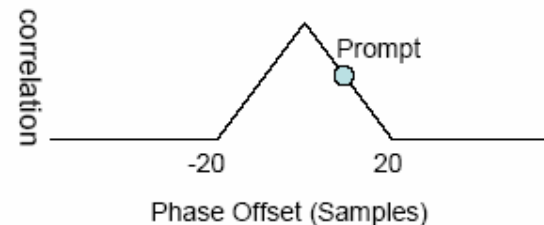


Figure 5.3 Correlation of C/A Code and an Input Signal with Phase Shift to the Right

Therefore, two additional sets of sampled C/A codes are needed to determine the direction of the shift. The two sets are the early and late codes respectively. The original sampled C/A code is referred as the prompt code. The early and late codes are time shifted versions of the prompt code by half a chip or less. In this case, the early copy of the C/A

code is shifted three samples to the left from the prompt code and the late code is shifted three samples to the right.

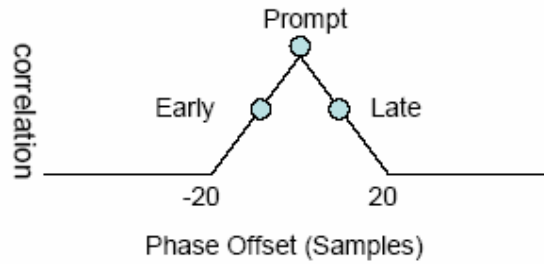


Figure 5.4 Correlation Plot of the Prompt, Early, and Late Codes

### 5.1.2 The Delay-Locked Loop (DLL)

The delay locked loop (DLL) consists of early, prompt and late code generators, filters and discriminators. The incoming IF signal is first down-converted by the carrier frequency obtained from the acquisition process to the  $I$  and  $Q$  channels at baseband. The down-conversion process can be described in Eq. 5.1 and Eq. 5.2

$$I = data \cdot \cos(2p \cdot f_c \cdot t) \quad Eq.5.1$$

$$Q = data \cdot \sin(2p \cdot f_c \cdot t) \quad Eq.5.2$$

where  $f_c$  is the IF carrier frequency estimated by the acquisition program. The  $I$  and  $Q$  channel data are multiplied by the early, late and prompt C/A codes to obtain the correlation values. The locally generated prompt signal is used to de-spread the incoming signal. The early and late codes each correlate with the incoming C/A coded signal to produce two other outputs. These outputs are filtered, squared and compared using a discriminator. Based on the discriminator output, if certain thresholds are crossed, the locally generated C/A code is adjusted to match the C/A code of the incoming signal. The sum of the  $I$  channel over one code period and the square envelope are given as follows

$$Ie = \sum(early * I) \quad Eq.5.3$$

$$ee = \sqrt{(Ie^2 + Qe^2)} \quad Eq.5.4$$

The sum of the envelopes is fed into the discriminator and then the code loop filter makes the decision if a phase change has occurred. Different discriminators can be used, for example, E-L envelope (which is used in the present algorithm), E-L power or E-L normalized. In the case of the Early-Late discriminator, the output signal  $e$ , is calculated

$$e = \frac{Early}{Late} \quad Eq. 5.5$$

The discriminator output is tested against two thresholds to see if a phase shift greater than the maximum tolerance has occurred in the receiver. From the output of the discriminator, the direction of the shift in the C/A code can be determined:



$e = 1$ , the prompt code is aligned with the incoming C/A coded signal, no shift is necessary,  
 $e < 1$ , a phase shift to the left has occurred, shift the codes to the right,  
 $e > 1$ , a phase shift to the right has occurred, shift the code to the left.

The discriminator output is averaged over 20 code periods. In the code loop filter, if the averaged result still crosses either threshold values, the codes are shifted accordingly. Figure 5.5 shows the block diagram of the code tracking loop.

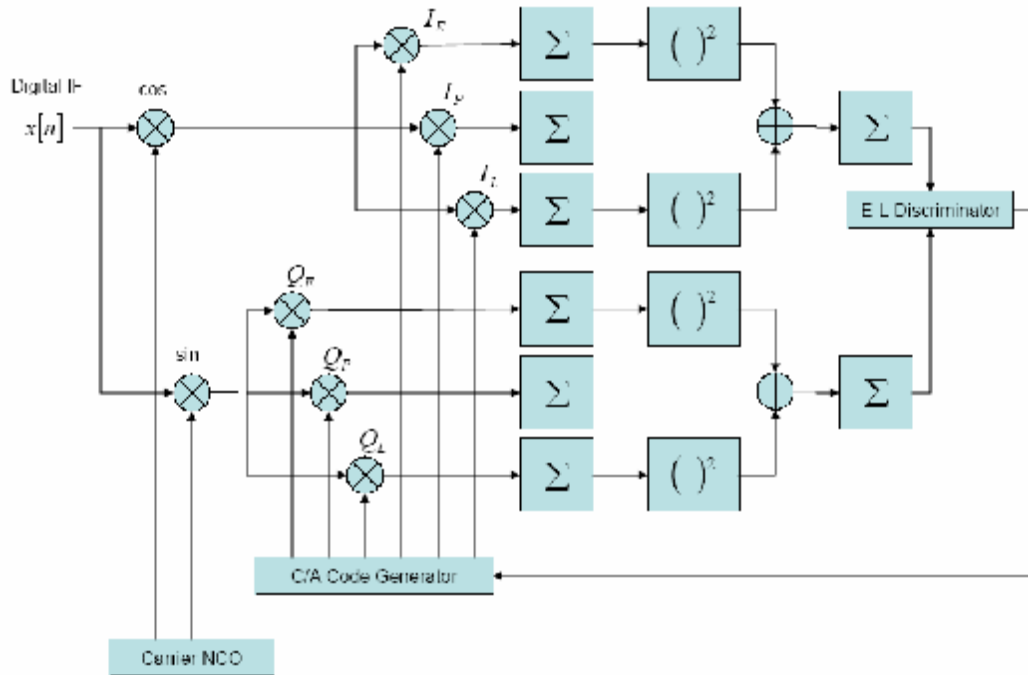


Figure 5.5 Block Diagram of Code Tracking Loop

## 5.2 Carrier Tracking

When the carrier frequency changes, the receiver loses track of the satellite signal. The carrier tracking process can keep phase lock of the satellite as long as the frequency shift is within the allowed range.

### 5.2.1 The Phase-Locked Loop (PLL)

The phase locked loop (PLL) is a critical component in coherent communications receivers that is responsible for locking onto the carrier of a received modulated signal [11]. Ideally the transmitted carrier frequency is known and its phase needs to be determined for accurate demodulation. However, due to factors such as noise and satellite motions, the actual carrier frequency received may be slightly different from the expected frequency. This difference can be modeled as a time-varying phase. Provided that the frequency mismatch is small relative to the carrier frequency, the feed-back control of an appropriately calibrated PLL can track this time-varying phase, thereby locking onto the correct frequency as well as phase [7].

The Phase Lock Loop (PLL) consists of a numerically controlled oscillator (NCO), carrier loop filter and a discriminator. The output of the DLL is a signal only modulated with

the navigation data, which is also used as the input to the PLL. The PLL used for GPS signal tracking is a Costas Loop. The output of the discriminator is used to generate a control signal to tune the frequency of the NCO so that the loop can continuously demodulate the incoming signal [8]. The PLL used to tracking a GPS signal is usually a second order loop. However, a higher order PLL is necessary for tracking signals on a high dynamics receiver [9].

The transfer function of the the second order loop filter in the z-domain can be described by the following equations

$$F(z) = \frac{(C1 + C2) - C1 * z^{-1}}{1 - z^{-1}} \quad \text{Eq. 5.6}$$

where  $C1$ ,  $C2$ ,  $w_n$ , and  $\Delta T$  are defined as

$$C1 = \frac{1}{K} \frac{8Vw_n\Delta T}{4 + 4Vw_n\Delta T + (w_n\Delta T)^2} \quad \text{Eq. 5.7, Eq. 5.8}$$

$$C2 = \frac{1}{K} \frac{4(w_n\Delta T)^2}{4 + 4Vw_n\Delta T + (w_n\Delta T)^2}$$

$$w_n = \frac{2b}{V + \frac{1}{4V}} \quad \text{Eq. 5.9, Eq. 5.10}$$

$$\Delta T = \frac{1}{1000} s$$

The parameter values of damping factor, natural frequency and loop gain are chosen according to the experimental results of [1]. The damping factor,  $V$ , a value of 0.707 is considered to be optimum. However, the change in natural frequency,  $w_n$  (which depends on the noise bandwidth), and loop gain affects success or failure of the tracking [6]. These parameters are related with the incoming signal strength. Normally a noise bandwidth of 20Hz and loop gain,  $K$  of 400 shall successfully track the incoming signal [1].

The carrier NCO generates an IF signal with the same frequency obtained from the acquisition program. The signal generated has both  $I$  and  $Q$  channels. The signal from each channel is correlated with the input signal and then lowpass filtered using an elliptic filter. An arc tangent (atan) discriminator that is insensitive to the phase transition of the navigation data bit transitions is used to determine the phase shift in the carrier frequency. Once the input IF signals in the  $I$  and  $Q$  channels are down-converted to baseband using the estimated carrier frequency  $f_c$ , the resulting baseband signals are then multiplied with the prompt code and are summed over one code period. The resulting  $I$  and  $Q$  signals are then fed into the discriminator which gives the angle in radians between the signals in the two channels. Figure 5.6 shows the schematics of the carrier tracking loop.

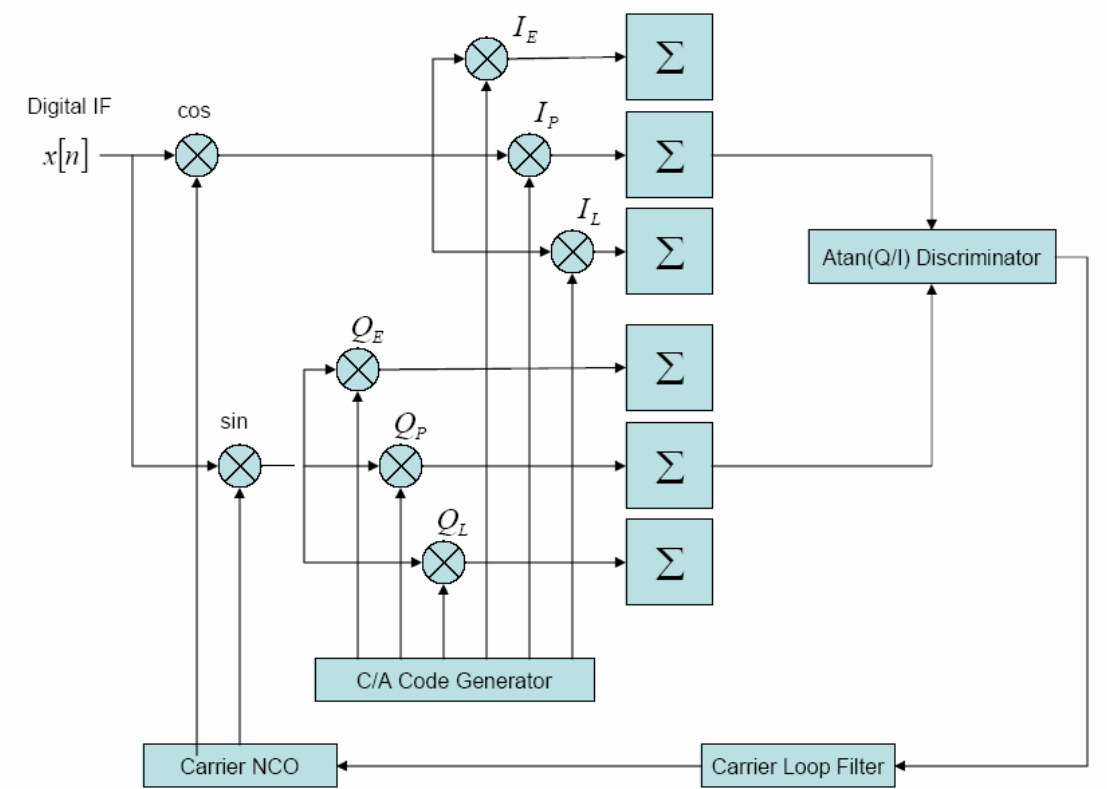


Figure 5.6 Block Diagram of Carrier Tracking Loop

The discriminator is an atan discriminator instead of an atan2 discriminator to take out the effect of phase shifts due to the BPSK modulation. The angle goes through the carrier loop filter to the carrier frequency NCO, in order to correct  $f_c$ . The correction of  $f_c$  is made by shifting the phase in a successive way. The corrected phase is calculated as

$$q_{corr} = q_{new} - q_{old}$$

### 5.3 GPS Signal Tracking Using the BASS Method

The conventional GPS receiver uses the DLL to track the shift in the C/A code and the PLL to track the carrier frequency. The combined block diagram of both the code and carrier tracking loops is shown in Figure 5.7.

In the case of a software GPS receiver, both loops are implemented in software. The tracking program for this software receiver uses the block adjustment of synchronizing signal (BASS) method. The DLL is still used to calculate the C/A code offset. The difference in the BASS method is that it uses one frequency component of the discrete Fourier transform to determine the phase of the carrier signal and uses consecutive measurements on phase to track the carrier frequency [11].

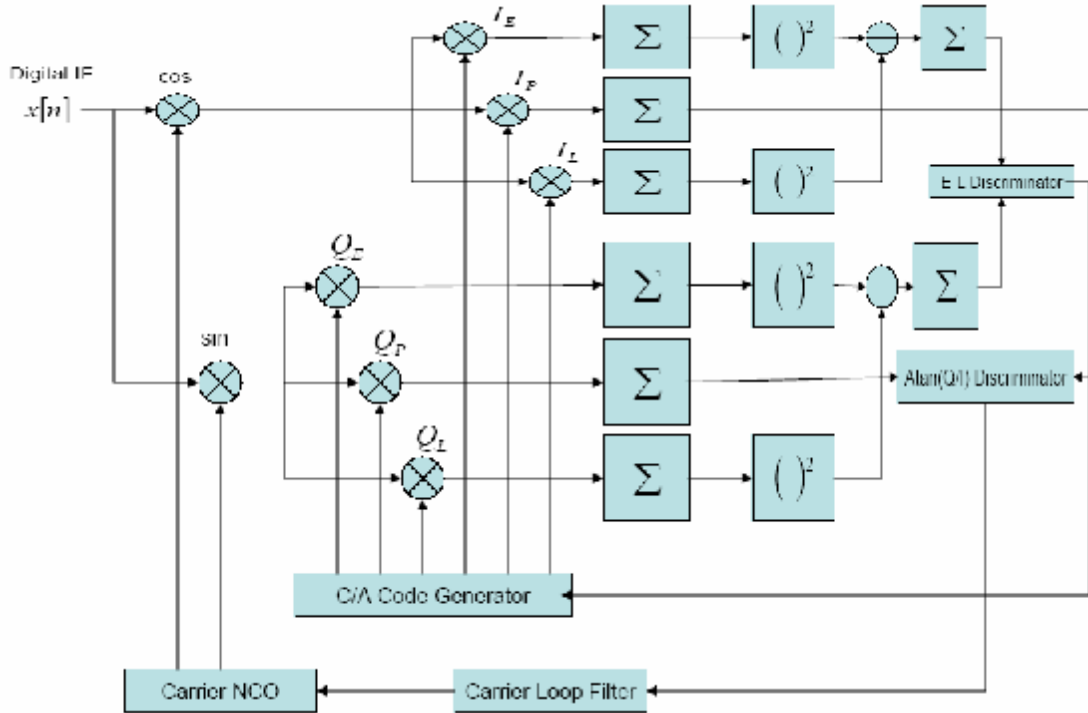


Figure 5.7 Block Diagram of Code and Carrier Tracking Loops

The incoming data is processed one millisecond at a time from the beginning of one set of C/A code. The input data is continually processed in millisecond increments by the tracking loops. Only one set of digitized C/A code is generated. The sampled C/A code is reused every millisecond with adjustments obtained from the output of the code tracking loop. Therefore, instead of generating a new set of C/A code and sample it for every block of input data, the C/A code samples can be reused to reduce the load on the processor. The locally generated carrier signal needs to be updated to the correct frequency for each set of input data.

The decoding of the navigation data only depends on the phase difference between two consecutive blocks of data. In order to create a continuous locally generated carrier, the initial phase of the data needs to be calculated. Adjustments to the carrier signal have to be made for every millisecond of data. The phase difference between the carrier signal and the input data over one millisecond should be either 0 or  $\pi$ , plus a constant bias as the phase error is not forced to zero. Ideally, the phase of the carrier signal and the C/A code should be synchronized [1]. In this initial development of the software receiver, this synchronization is overlooked to reduce the complexity of the system.

The DFT of the input signal,  $x(n)$ , is defined as

$$X(k) = \sum_{n=0}^{N-1} x(n) e^{-j2\pi kn/N} \quad \text{Eq. 5.11}$$

where  $k$  is the  $k$ -th frequency component of the input signal and  $N$  is the total number of data points. The frequency component with the highest amplitude,  $|X(k_i)|$ , is the frequency of the incoming signal. The initial phase of the block of data can be calculated using Eq. 4.11. This

operation is repeated for the highest frequency component of each millisecond of data. The fine frequency can be obtained from Eq. 4.13.

Similar to the acquisition process, the performance of the tracking program is first verified on the MATLAB simulated GPS data. The spectrum of one millisecond of the incoming C/A coded signal at IF is shown in Figure 5.8. From visual observation, it is very similar to the signal in Figure 3.10 (they should theoretically be identical).

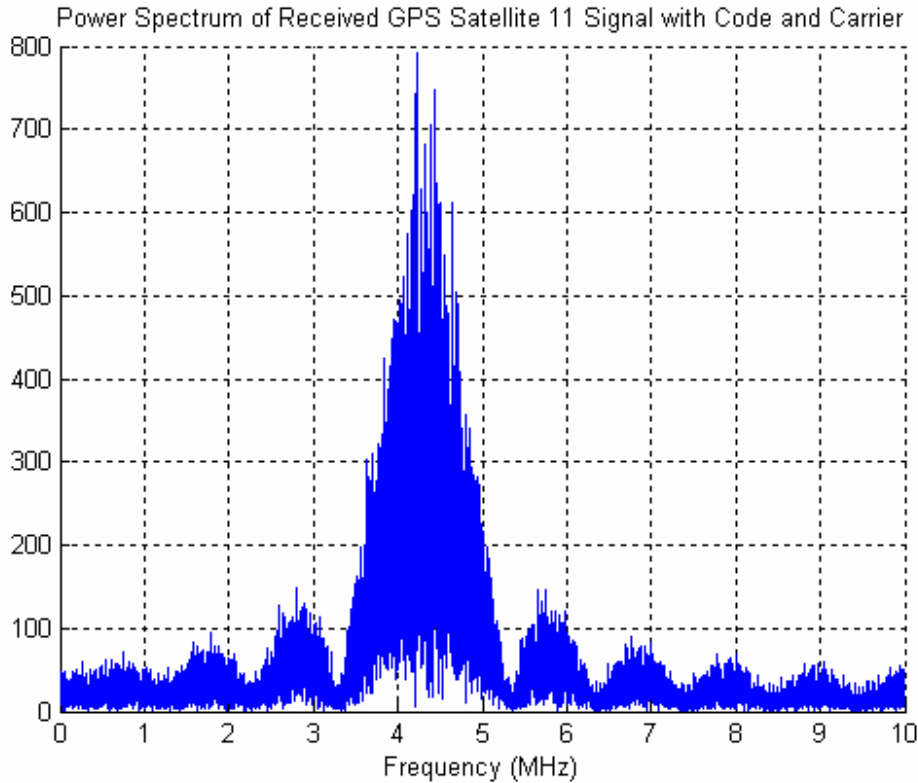


**Figure 5.8 Spectrum of Received GPS C/A Coded Data for Satellite 11 at IF**

The spectrum of the same data after the C/A code has been removed is shown in Figure 5.9. The frequency of the highest component is at approximately 4.3 MHz, which corresponds to the range of the input carrier frequencies. Once the C/A code is despread, only the carrier frequency is modulated on the data signal.

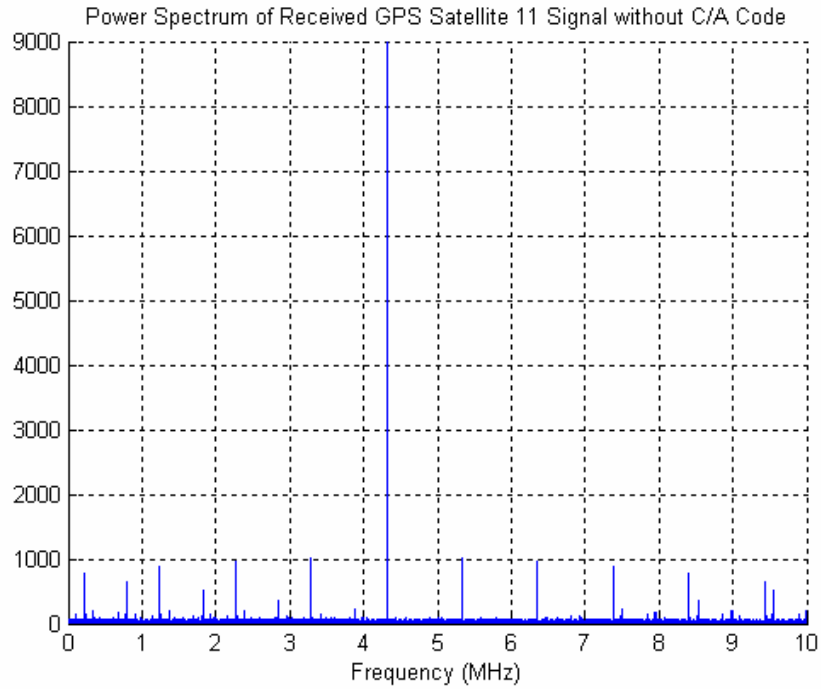


**Figure 5.9 Spectrum of Received GPS Signal for Satellite 11 with C/A Code Removed**

For testing purposes, the original one millisecond of input data is first demodulated by the carrier frequency obtained from the acquisition program with the C/A code still in the signal. From Figure 5.10, it can be seen that the bandwidth of the mainlobe of the spectrum is approximately 2 MHz. This result matches the bandwidth of the C/A code.

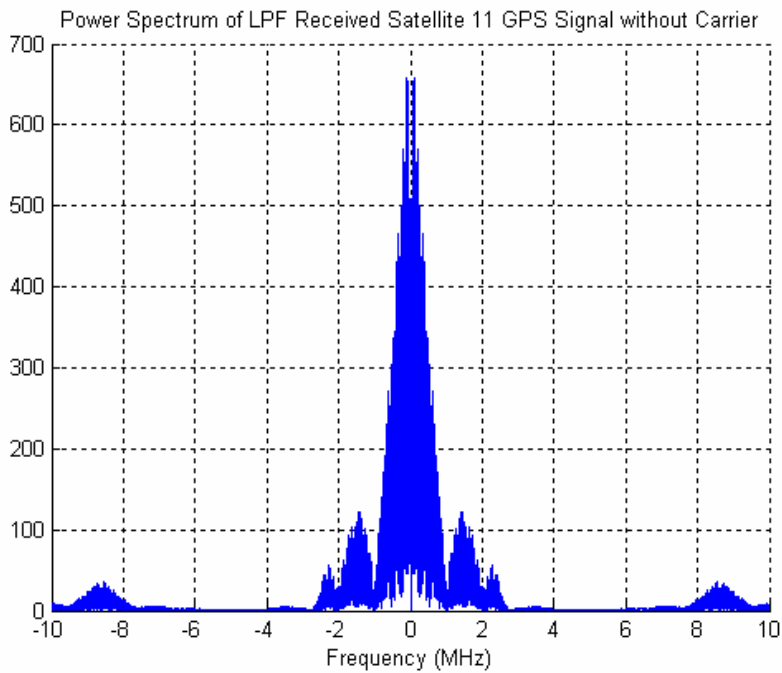


**Figure 5.10 Spectrum of Received GPS Signal for Satellite 11 with C/A Code at Baseband**

The one millisecond of data after despreading and demodulation is shown in Figure 5.11. The frequency of the navigation data should be at baseband. This process is repeated for all 10 data bits simulated, which lasts 200 ms. The recovered data bits from the tracking program are illustrated in Figure 5.12. The results match the waveform of the original simulated input data bits.

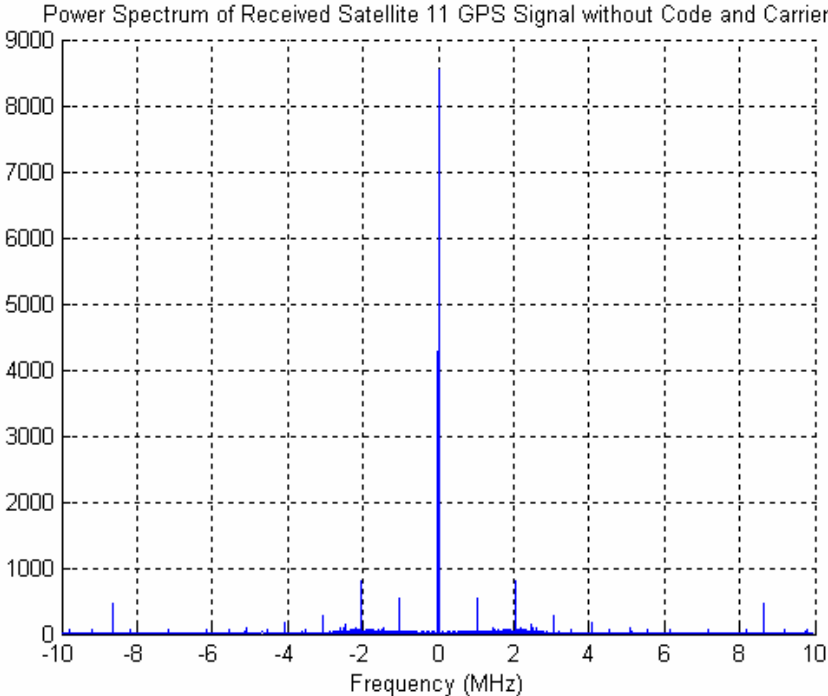


**Figure 5.11 Spectrum of Received GPS Signal for Satellite 11 at Baseband**

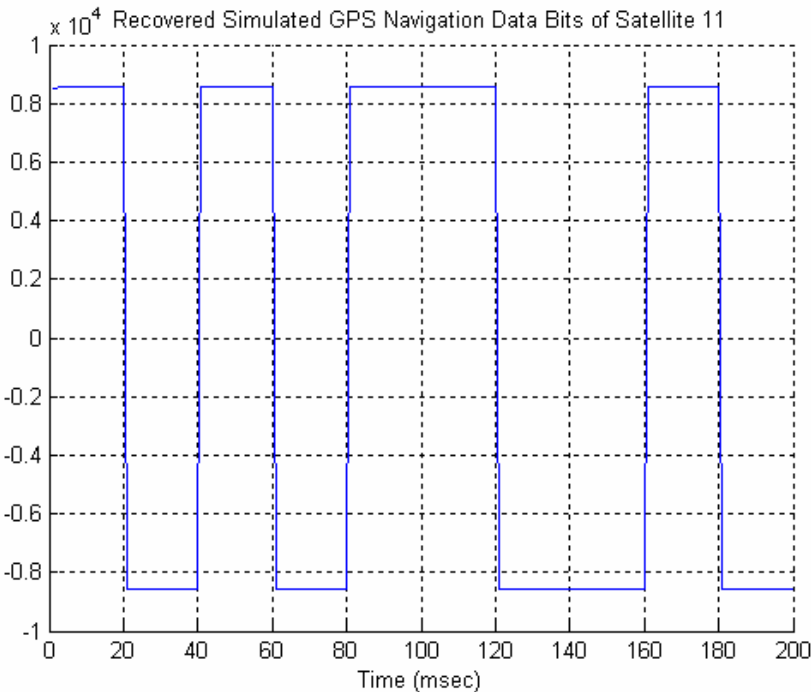


**Figure 5.12 Recovered GPS Navigation Data Bits for Satellite 11**

The real-like signal from the simulator is then tested using the tracking program. For a comparison with the simulated data, the spectrum of the first one millisecond of data is also plotted in Figure 5.13. The signal is noisier than the simulated signal and the magnitude of the spectrum is much smaller because the input signal is very weak.

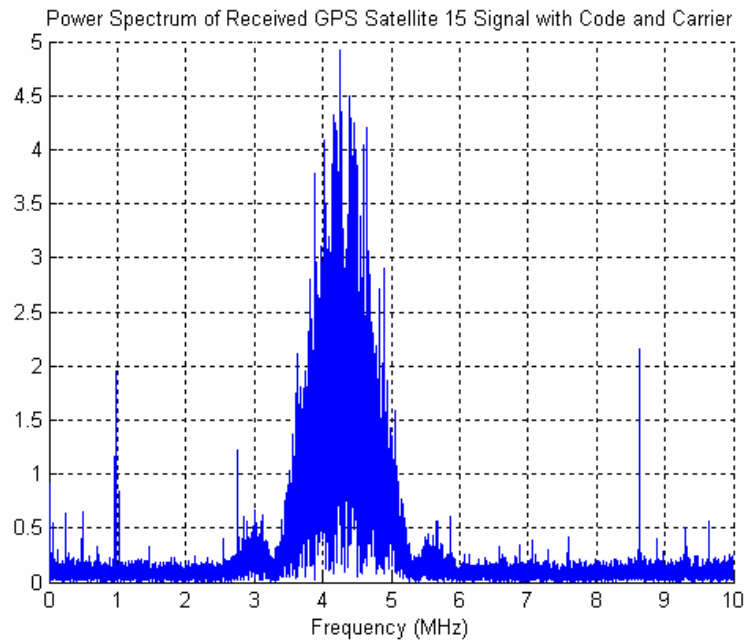


**Figure 5.13 Spectrum of Received GPS C/A Coded Data for Satellite 15 at IF**

After the C/A code is stripped off the incoming signal, the data is still modulated by the carrier frequency. The frequency of the signal also at approximately 4.3 MHz (see Figure 5.14). The original signal is also down-converted to baseband using the carrier frequency from the acquisition program with the C/A code. The result is filtered and shown in Figure 5.15.

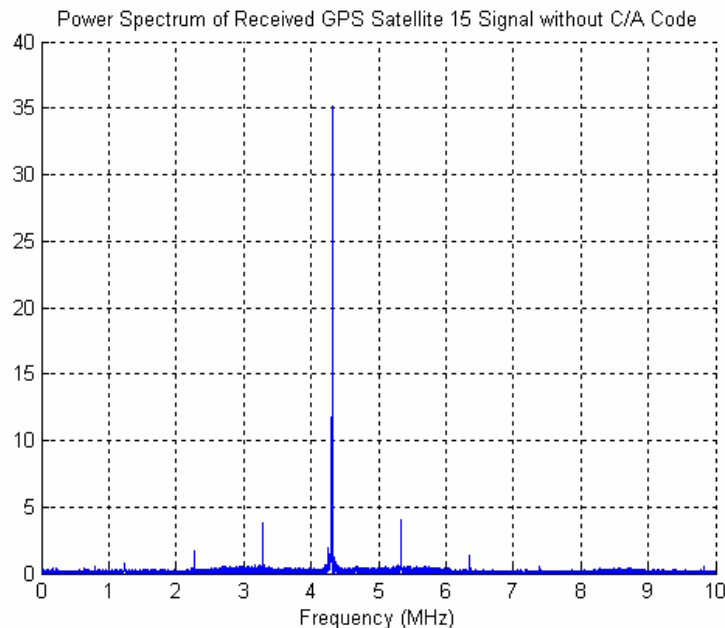


**Figure 5.14 Spectrum of Received GPS Signal for Satellite 15 with C/A Code Removed**



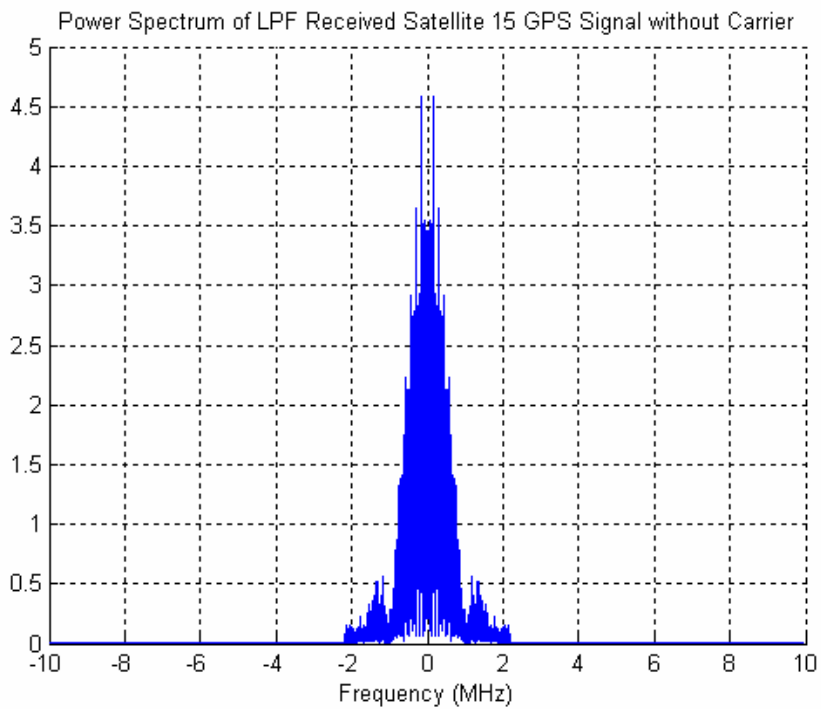


**Figure 5.15 Spectrum of Received GPS Signal for Satellite 15 with C/A Code at Baseband**

The spectrum of the first millisecond of signal without C/A code and carrier frequency is at baseband and plotted in Figure 5.16.

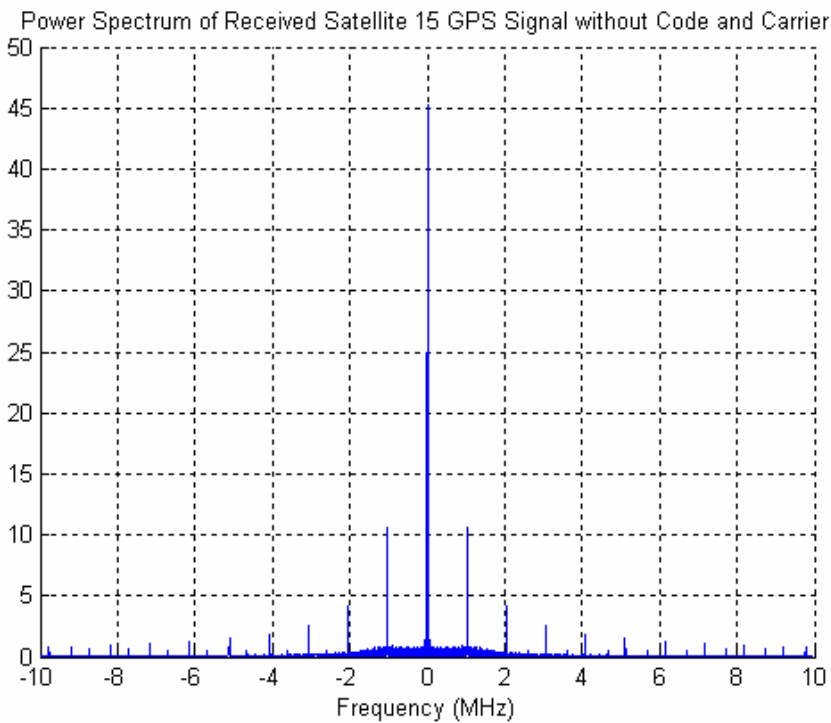


**Figure 5.16 Spectrum of Received GPS Signal for Satellite 15 at Baseband**

The tracking output of two seconds of data is shown in Figure 5.17. Compared to the navigation data bits recovered from the simulated data, the magnitudes of these data bits are much smaller due to the weak input signal. The carrier frequency does not seem to be completely removed because the weaker signal is much more sensitive to frequency shift. A more detailed view of the recovered bits is shown in Figure 5.18 for 400ms. The bit transitions can be seen clearly and each bit lasts approximately 20 ms which corresponds to the length of a data bit.

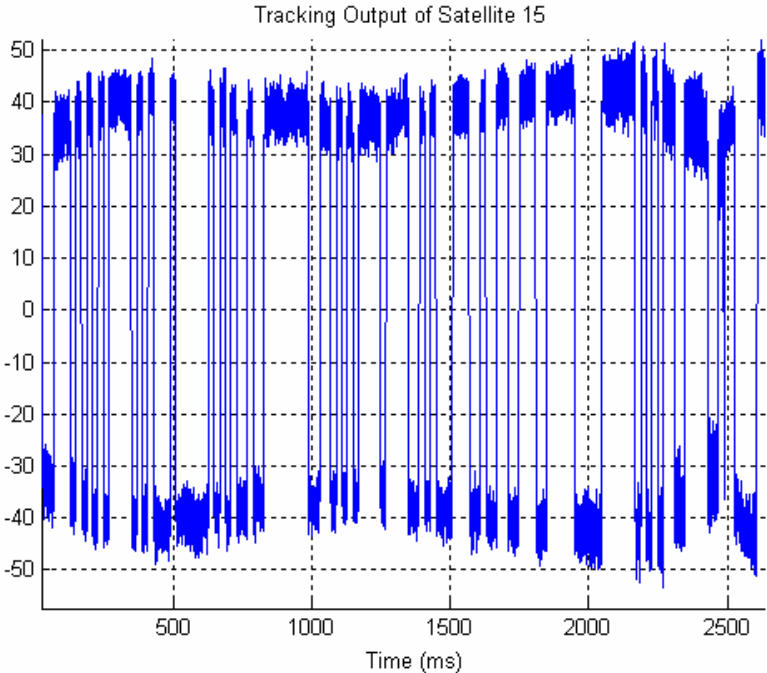


**Figure 5.17 Recovered GPS Navigation Data Bits for Satellite 15**

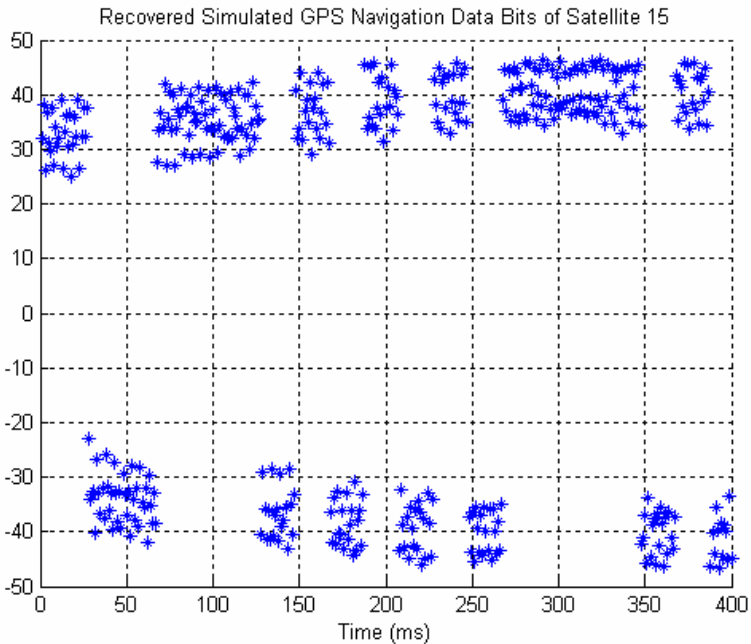


**Figure 5.18 a Recovered GPS Navigation Data Bits for Satellite 15 for 400 ms**

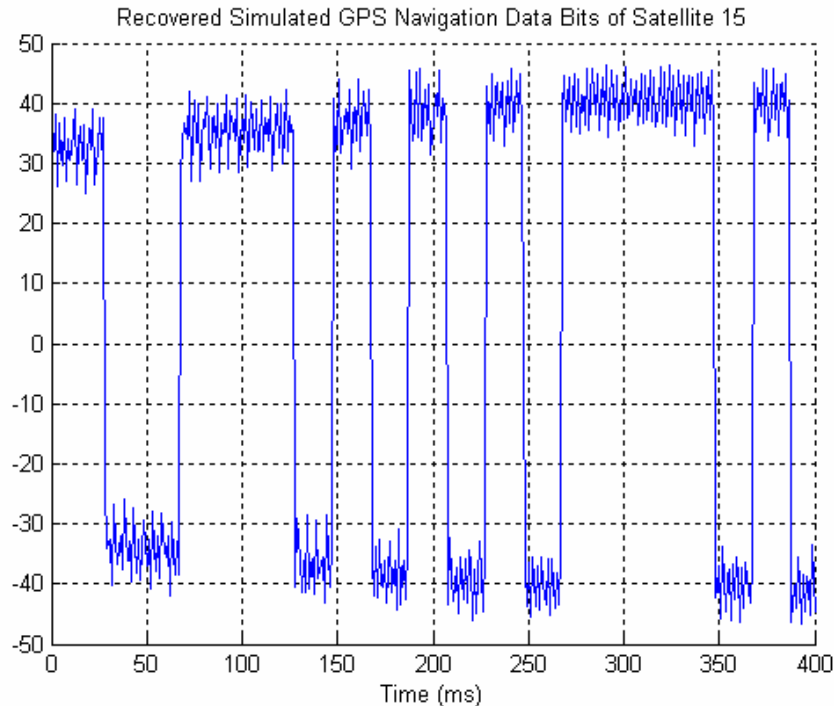


**Figure 5.18 b Recovered GPS Navigation Data Bits for Satellite 15 for 400 ms**

## CHAPTER 6 FUTURE WORK

The acquisition and tracking programs presented above are written specifically for this ongoing development of the software GPS receiver. Both programs are tested for both MATLAB simulated data and GSS 6560 simulated data. Scenarios were designed using SimGEN to create the simulated GPS data. The resulting IF signal is extracted from the Mitel 2021 board and then digitized. The data from the simulator data is much weaker in magnitude. The quantization levels of the 8-bit UltraFast 2020 board maybe insufficient for accurate signal representations. The signals are easily lost in the tracking loops due to quantization noise. For future work, an amplifier can be installed between the output of the Mitel 2021 board and the ADC. The BASS method is used to recover the navigation bits instead of the conventional PLL. To recover longer periods of navigation data, modifications to the hardware setup have to be made. The memory of the computer used to digitize the data needs to be increased to take longer periods of data. The current configuration can only take a maximum of 10 seconds of data. Also the future code should be converted to C to improve data processing efficiency. Once longer periods of data can be obtained, the navigation messages can be decoded by comparing the recovered data with the parity bits.

The goal of the complete development of the software receiver is to be able to track real-time GPS signals in the future. Also with the development of new GPS signals at the L5 frequency, the acquisition and tracking programs software receiver can be tested at the new frequency. Since the code can also be adapted in the future for possibly testing the new Galileo system developed by the European Union. As long as the code structures are known, the programs can also be modified to decode the P code and the newly developed M code in the future.

## LIST OF REFERENCES

- [1]. Tsui, James Bao-Yen, *Fundamentals of Global Positioning System Receivers: A Software Approach*, John Wiley & Sons, Inc. 2000.
- [2]. Misra P., P. Enge, *Global Positioning System: Signals, Measurements, and Performance*, Ganga-Jamuna Press, 2001.
- [3]. Kaplan, E., *Understanding GPS: Principles and Applications*, Norwood, MA, Artech House, 1990
- [4]. Spirent Communications Limited, *SimGEN USER MANUAL*, Issue 1-08, January 2004.
- [5]. Akos, D., A Software Radio Approach to Global Navigation Satellite System Receiver Design, Ph. D. Dissertation, Ohio University, 1997
- [6]. Litwin, Louis, *Matched Filtering and Timing Recovery in Digital Receivers: A practical look at methods for signal detection and symbol synchronization*. RF Design. September, 2001.
- [7]. Jovanovic, V.M., Analysis of Strategies for Serial-Search Spread-Spectrum Code Acquisition-Direct Approach, IEEE Transactions on Communications, Vol. COM-36, No.11, November 1988, pp. 1208-1220
- [8]. Parkinson, Bradford, and Spilker, Jr., James. *Global Positioning System: Theory and Applications*. Vol. I.
- [9]. <http://shiba.iis.u-tokyo.ac.jp/member/current/dinesh/index.htm>
- [10]. Proakis, J. G., *Digital Communications*. McGraw-Hill, 3rd ed., 2001.
- [11]. Gaby M. Neunzert, *Global Positioning*, Golden Colorado, 1999.